Universidade do Minho
Escola de Medicina

Marta Sofia Carvalhal Monteiro

The potential role of innate immune memory in Multiple Sclerosis disease using autoimmune experimental encephalomyelitis mouse model

julho de 2019

The potential role of innate immune memory in Multiple Sclerosis disease using autoimmune experimental encephalomyelitis mouse model
Marta Sofia Carvalhal Monteiro
UMinho|2019

Universidade do Minho
Escola de Medicina

Marta Sofia Carvalhal Monteiro

The potential role of innate immune memory in Multiple Sclerosis disease using autoimmune experimental encephalomyelitis mouse model

Dissertação de Mestrado
Mestrado em Ciências da Saúde

Trabalho efetuado sob a orientação da
Professora Doutora Fernanda Marques
e do
Professor Doutor João Cerqueira

julho de 2019

Agradecimentos

À Fernanda e ao João, pela orientação, compreensão e ajuda. Pela oportunidade de aprender e crescer, como pessoa e como profissional. Foram, sem dúvida, pilares essenciais para que a realização desta tese fosse possível.

À Sofia e à Joana que acima de colegas de laboratório, foram verdadeiras companheiras durante esta jornada. Obrigada pela amizade, apoio, conhecimento, pelos momentos de gargalhada e interajuda. É com emoção e carinho que vos agradeço.

Aos meus colegas do Mestrado em Ciências da Saúde, estes anos serão sempre lembrados com a vossa presença. É com orgulho que revejo todo este duro caminho ao lado de pessoas tão brilhantes, tenho a certeza que o sucesso vos espera!

A todos os outros colegas com quem compartilhei momentos de verdadeira amizade e aprendizagem, Marco, Inês, Margarida, Bárbara, Madalena, Caroline e Catarina, o meu mais sincero obrigada. Fizeram com que me sentisse sempre integrada e bem-vinda.

A todos os NeRD, pela ajuda e pelas sugestões.

Aos meus amigos, Catarina, Bruna, Joana, Eliana, Andreia, Sofia, Mónica, Márcia, Nuno, Miguel, Ana, Rui, Sofia e Mendanha. Obrigada por todo o companheirismo e paciência. Obrigada por não me deixarem ir abaixo, pelas vossas palavras de motivação e por ouvirem os meus lamentos. Obrigada pelas gargalhadas, e pelos sorrisos. Obrigada com o maior amor do mundo!

Aos meus pais, irmã e cunhado. Obrigada por todos os dias me ensinarem a ser mais forte, e a nunca desistir. Obrigada pelos conselhos, pelo colo e por me fazerem ver que o amor verdadeiro está sempre lá para nós. Obrigada sobretudo aos meus pais, pelo árduo esforço de fazerem de mim o que sou hoje, sou orgulhosa por ser vossa filha. Amo-vos a todos do fundo meu coração.

Ao Tiago, obrigada sobretudo pela paciência, mesmo com o mau feitio. Obrigada por acreditares em mim, e me relembrares isso todos os dias. Obrigada por dares sentido a cada gargalhada e a cada lágrima. Obrigada por lutares comigo, e por dares luta. Obrigada pelo amor, mas sobretudo pela amizade. Amo-te meu bem.

O trabalho apresentado nesta tese foi realizado no Instituto de Investigação em Ciências da Vida e Saúde (ICVS), Universidade do Minho. O financiamento é proveniente dos Fundo Europeu de Desenvolvimento Regional (FEDER) através Programa Operacional Factores de Competitividade – COMPETE, e dos fundos nacionais através da Fundação para a Ciência e Tecnologia sobre POCI-01-0145-FEDER-007038; e sobre o projeto NORTE-01-0145-FEDER-000013 do Programa Operacional Regional do Norte (NORTE 2020), sobre o Acordo de Parceria PORTUGAL 2020, através da FEDER.

STATEMENT OF INTEGRITY

I hereby declare having conducted this academic work with integrity. I confirm that I have not used plagiarism or any form of undue use of information or falsification of results along the process leading to its elaboration.

I further declare that I have fully acknowledged the Code of Ethical Conduct of the University of Minho.

O potencial papel da memória da imunidade inata na doença da esclerose múltipla usando o modelo de ratinho encefalomielite autoimune experimental

Resumo

Estudos recentes demonstraram que a memória imune também está presente nas células do sistema imune inato. No cérebro, esta memória imune inata é predominantemente mediada pela microglia, e foi demonstrado que, diferentes regimes de injeções periféricas com um componente da membrana externa de bactérias Gram-negativas, o lipopolissacarídeo (LPS), são capazes de induzir fenótipos distintos na microglia: "treinada" ou "tolerante". Neste contexto, foi recentemente demonstrado que o "treino" imunológico promove a patologia da doença de Alzheimer e do acidente vascular cerebral, enquanto que a "tolerância" alivia estas condições. No entanto, nada é sabido sobre o seu impacto na esclerose múltipla. Assim sendo, neste trabalho, a hipótese é que a modulação destas células para um fenótipo mais "tolerante" (4X LPS) em termos imunológicos poderá promover neuroprotecção e diminuir a resposta inflamatória associada à esclerose múltipla. Para isso, foi administrada em fêmeas C57BL/6 uma única injeção de LPS para induzir o "treino" (1X LPS) imunológico ou quatro injeções consecutivas de LPS para induzir uma "tolerância" (4X LPS) imunológica. Um mês depois, estes animais foram induzidos com a encefalomielite autoimune experimental (EAE), um dos modelos animais de esclerose múltipla mais estudados, e foram posteriormente sacrificados no pico (dia 17) e na fase crónica da doença (dia 29), juntamente com os controlos não induzidos. Em relação ao score clínico dos animais, não encontramos diferenças significativas no desenvolvimento da doença nos animais injetados com LPS, demonstrando que o pré-tratamento com LPS não estão a influenciar o aparecimento e desenvolvimento da doença. Apesar desta observação, a nível molecular verificamos que animais EAE expostos a um estimulo que induz o "treino" imunológico expressam mais interleucina *(Il)-6* e *Gfap* na fase do pico da doença, e uma maior percentagem de áreas de lesão na fase crónica da doença, em comparação com animais EAE expostos a um estimulo que induz a "tolerância" imunológica e com animais EAE controlo.

Em suma, este trabalho sugere que uma modulação da memória das células imunes inatas residentes no sistema nervoso central pode ter um leve papel na patogenicidade da doença, sem ter um impacto na severidade da doença. No entanto estudos futuros são necessários para se perceber melhor sobre os mecanismos que poderão estar subadjacentes ao "treino" e "tolerância" imunológica no modelo EAE e na esclerose múltipla.

Palavras-chave: Astrócitos; EAE; Esclerose Múltipla; Memória da imunidade inata; Microglia.

The potential role of innate immune memory in multiple sclerosis disease using experimental autoimmune encephalomyelitis mouse model

Abstract

Recent studies showed that immune memory is also present in the cells of the innate immune system. In the brain, this innate immune memory is predominantly mediated by microglia, and it was demonstrated that, different regiments of peripheral injection of lipopolysaccharide (LPS), which is a component derived from the outer membrane of Gram-negative bacteria, are able to induce microglia immune training or tolerance. In this context, it was recently shown that immune training promotes Alzheimer's disease (AD) and stroke pathology, while tolerance alleviates these conditions. However, nothing is known about its impact in multiple sclerosis (MS). Therefore, in this work, we hypothesized that modulation of these cells towards immune tolerance could also promote neuroprotection and reduce disease burden. For that, we gave to C57BL/6 females a single intraperitoneal injection of LPS to induce training (1X LPS) and four consecutive injections of LPS to induce tolerance (4X LPS). One-month later, these animals were challenged with experimental autoimmune encephalomyelitis (EAE) – one of the most studied animal models of MS – and were sacrificed at the onset (day 17) and at the chronic phase of the disease (day 29), along with non-induced controls. Herein, we analyzed the disease course of EAE animals, showing that the LPS pretreatment conditions are not influencing the overall disease development. Nevertheless, we observed that animals exposed to a training-induced stimulus (1X LPS) expressed more interleukin *(Il)-6* and glial fibrillary acidic protein *(Gfap)* at the onset phase of disease, and a higher percentage of lesioned areas at the chronic phase of disease, in comparison to EAE animals exposed to a tolerance-induced stimulus (4X LPS) and to EAE control animals.

In summary, this work suggests that modulation of central nervous system resident innate immune cells memory may play a slightly role in disease pathogenesis, without having an impact on disease severity. This may provide insights for further investigation on the mechanisms behind this acute immune training and acute immune tolerance in EAE model.

Key words: Astrocytes; EAE; Innate immune memory; Microglia; Multiple Sclerosis.

Index

Abbreviations

A

AD	Alzheimer's disease
APC	Antigen presenting cell
ATP	Adenosine triphosphate
ATP5B	ATP F1 subunit beta mitochondrial

B

BBB	Blood-brain-barrier
BCG	Bacillus Calmette-Guérin

C

cDNA	Complementary DNA
CFA	Complete Freund's adjuvant
CIS	Clinically isolated syndrome
CNS	Central nervous system
CSF	Cerebrospinal fluid
CX3CR1	CX3C chemokine receptor 1

D

DAM	Disease-associated microglia
DNA	Deoxyribonucleic acid

E

EAE	Experimental autoimmune encephalomyelitis
EBV	Epstein Barr virus
ECM	Extracellular matrix
EDTA	Ethylenediamine tetraacetic acid
EtBr	Ethidium bromide

F

FBS	Fetal bovine serum

G

GFAP	Glial fibrillary acidic protein
GWAS	Genome-wide association studies

H

HIF	Hypoxia inducible factor
HLA	Human leukocyte antigen
HSPCB	Heat shock 90kD protein 1 beta

I

IBA1	Ionized calcium-binding adapter molecule 1
ICAM	Intercellular adhesion molecule
IFN	Interferon
Ig	Immunoglobulin
IL	Interleukin
ILC	Innate lymphoid cell
iNOS	Inducible nitric oxide synthase

L

LCN2	Lipocalin 2
LFA	Lymphocyte function-associated antigen
LPS	Lipopolysaccharide

M

MAPK	Mitogen-activated protein kinase

MBP	Myelin basic protein
MHC	Major histocompatibility complex
MOG	Myelin oligodendrocyte glycoprotein
MMP	Matrix metalloproteinase
MRI	Magnetic resonance imaging
MS	Multiple sclerosis
NAWM	Normal appearing white matter

N

NK	Natural killer

O

OPC	Oligodendrocyte progenitor cell

P

P2RY12	Purinergic receptor P2Y
PBS	Phosphate buffer solution
PCR	Polymerase chain reaction
PFA	Paraformaldehyde
PLP	Proteolipid protein
PRR	Pattern recognition receptor
PP-MS	Primary progressive MS
PR-MS	Progressive relapsing MS
PTX	Pertussis toxin

Q

qRT-PCR	Quantitative real-time PCR

R

RM	Repeated measures
ROS	Reactive oxygen species
RNA	Ribonucleic acid
RNS	Reactive nitrogen species
RR-MS	Relapsing remitting MS
RT	Room-temperature

S

SCH	Spinal cord homogenates
SEM	Standard error of the mean
SNT	Simple neurite tracer
SP-MS	Secondary progressive MS

T

TCA	Tricarboxylic acid cycle
TCR	T-cell receptor
TET	Ten-eleven translocation
TFAIP3	Tumor necrosis factor, alpha-induced protein 3
Th	T helper
TLR	Toll-like receptor
TMEM 119	Transmembrane protein 119
TMEV	Theiler's murine encephalomyelitis virus
TNF	Tumor necrosis factor
Treg	T regulatory
TREM	Triggering receptor expressed on myeloid cells

V

VCAM	Vascular cell adhesion molecule
VLA	Very late antigen

Figure index

Tables index

1. Introduction

1.1. Multiple Sclerosis: Disease overview

In the middle-end of the XIX century (1868), the French neurologist Jean-Martin Charcot made the first description of multiple sclerosis (MS) under the name "*La Sclérose en Plaques*". His greatest contribution was to identify diagnostic criteria, although these were later revised. Charcot research was strongly based on the personal diary of Augustus d'Este (1794-1848), a men who carefully described his illness, becoming the first recognizable case of MS in the world (Fazio, Fredrikson, & Granieri, 2010).

Nowadays, MS is known as a chronic inflammatory autoimmune demyelinating disease of the central nervous system (CNS), that affects approximately 2.5 million people worldwide (Figure 1) (Browne, Tremlett, Baker, & Taylor, 2014).

Figure 1 - Prevalence of MS in a worldwide perspective. MS is one of the world's most common neurological disorder, affecting almost 2,5 million people. The predominant age to be diagnosed is between 20 and 40 years old however, people can be diagnosed at any age. Also, MS is twice more common among women

than men, which is not yet fully understood. Although the current efforts, MS is still a prevalent disease that cannot be cure.

The pathogenesis of MS involves the development of an abnormal immune response against the CNS myelin (a lipid-rich substance that insulates nerve cell axons), the specialized cells that produce myelin, as well as the nerve fibers themselves (Peferoen, Kipp, van der Valk, van Noort, & Amor, 2014). Consequently, the communication between neurons is altered or interrupted, which will lead to accumulation of disability in patients. This condition carries an enormous personal and socioeconomical burden since the average age of disease onset is 30 years, a time that is crucial for work and family planning (Figure 1) ((Dendrou, Fugger, & Friese, 2015).

Most patients display a clinically isolated syndrome (CIS) in young adulthood. These CIS patients present an acute episode of neurologic symptoms caused by inflammation and demyelination in the CNS, particularly in the optic nerves, brainstem, spinal cord or cerebellum (Miller, Chard, & Ciccarelli, 2012). This episode is characteristic of MS but does not yet meet the final MS diagnosis. For a patient to be considered with MS, he or she needs to fulfill the McDonald criteria, which are the clinical, radiographic, and laboratory criteria used in the diagnosis of MS. They were originally introduced in 2001 and revised multiple times, most recently in 2017, and they require lesion dissemination in space and time. The diagnosis of definite MS is based on the available diagnostic criteria with support of two different techniques routinely used in clinical practice, magnetic resonance imaging (MRI) of the CNS and cerebrospinal fluid (CSF) analysis (A. J. Thompson et al., 2018). Concerning MRI findings, the presence of multifocal demyelinating lesions at different timepoints in the white matter of the CNS (spatiotemporal dissemination criterion) are indicative of MS (Goldenberg, 2012; A. J. Thompson et al., 2018). Besides this, the presence of oligoclonal bands or increased concentration of immunoglobulin (Ig) G in the patients CSF (inflammatory criterion) also supports MS diagnosis (Goldenberg, 2012; Sankowski, Mader, & Valdés-Ferrer, 2015), but are not MS-specific (Greve, Enzmann, & Hosser, 2014).

Patients diagnosed with definite MS can exhibit different clinical forms, and present highly varied symptoms along time. The variation on these clinical manifestations are correlated with the spatiotemporal dissemination of lesioned sites of pathology in the CNS (Miljković & Spasojević, 2013). The most common include sensory symptoms (paresthesia), motor spinal cord symptoms (numbness and weakness), cerebellar symptoms (ataxia and tremor), fatigue, optic neuritis and other eye symptoms (blurred or double vision) (Ghasemi, Razavi, & Nikzad, 2017; Goldenberg, 2012). However, as the disease progresses, patients start to develop symptoms related to autonomic nervous system, namely bladder,

bowel and sexual dysfunction (Ghasemi et al., 2017). Ultimately, 60% of MS patients became confined to a wheelchair 20 years after onset (Our, 2013).

In the past years, efforts to categorize patients by general patterns of disease presentation allowed the recognition of several disease subtypes. The most common form, affecting 80%-85% of patients, is the relapsing remitting MS form (RR-MS) (Compston & Coles, 2008). RR-MS is characterized by acute attacks of new or increasing neurologic deficits – called relapses – followed by periods of clinical recovery (remission) (Dendrou, Fugger, & Friese, 2015). However, 80% of RR-MS patients loses the ability to recover from relapses with time (Dendrou, Fugger, & Friese, 2015). Consequently, the persistent symptoms accumulate, leading to a phase of progressive neurological deterioration termed secondary progressive MS (SP-MS). Approximately 15-20% of patients has primary progressive MS (PP-MS), a condition characterized by gradually worsening of the symptoms since the onset of the disease (Dendrou et al., 2015). A minority of the patients, 5%, present since their onset a progressive relapsing form (PR-MS) which is also characterized by relapses but, between those relapses the disease continues to get worse slowly.

Noteworthy, although some CIS patients fully recover without any intervention, other patients go on to develop MS. During the last years, there has been much interest and research in CIS patients, focusing on better understanding the cause and pathogenesis. Studies have aimed to improve the diagnostic criteria and the available disease-modifying treatments, encouraging more accurate diagnosis and early treatments to delay the development from CIS to MS. Currently, improvements in MRI technology already better allow the identification of the CIS patients that present a high or low risk of having a future episode (Marcus & Waubant, 2013). Also, CIS patients that were considered at high risk may now be treated with disease-modifying treatments approved by the U.S. Food and Drug Administration for that purpose (Marcus & Waubant, 2013).

1.2. Etiology of MS disease

1.2.1. Genetic and environmental factors

Although the etiology of MS disease remains to be elucidated, environmental factors, such as exposure to infectious agents and lifestyle, and genetic factors have been thought to contribute to the initiation and maintenance of chronic and exacerbated inflammation (Correale, Gaitán, Ysrraelit, & Fiol, 2016). Regarding the infectious agents, Epstein Barr virus (EBV), human herpes virus type 6, and mycoplasma pneumonia are the most studied contributors (Loma & Heyman, 2011). It is hypothesized that these

pathogens may have antigens structurally homologous with myelin sheet components (Ghasemi et al., 2017), like myelin basic protein (MBP), proteolipid protein (PLP) and myelin oligodendrocyte glycoprotein (MOG). In that way, when immune cells are activated by these pathogens, they may latter mount an immune response against the structurally similar myelin peptides, leading to the formation of demyelinating lesions.

Among lifestyle factors, vitamin D deficiency has been recognized as a potential risk factor for MS. According to previous reports, low sunlight exposure, and consequently, low vitamin D3 levels, could have a relationship with the incidence of MS (Ghasemi et al., 2017). Specifically, it was demonstrated that vitamin D3 via induction of T regulatory (Treg) cells and anti-/pro-inflammatory cytokines such as interleukin (IL)-10 and tumor necrosis factor (TNF)-alpha, may have immunomodulatory effects in MS.

In the field of the genetic factors, it is known that the risk of MS in family members of a patient depends on the amount of genetic information they share (Ghasemi et al., 2017). Accordingly, genome-wide association studies (GWAS) have shown that the human leukocyte antigen (HLA) locus on chromosome 6, which contains the DR antigens, is linked to MS susceptibility (Loma & Heyman, 2011). Specifically, the allele HLA-DRB1*15, of the class II gene HLA-DRB1, was identified as the haplotype that represents the highest risk factor for MS (Sankowski et al., 2015). However, susceptibility in non-HLA loci was also identified as being associated with MS, such as the genes encoding the α-chains of the IL-2 and IL-17 receptors (*IL-2RA* and *IL-7RA*, respectively) (Dendrou et al., 2015). Thus, overall the majority of MS associated genes are involved in the immunological response, which is not surprisingly due to the strong inflammatory component of this disease.

1.2.2. Mechanisms underlying disease

The pathologic hallmark of MS is the formation of plaques, which represents the end stage of a process involving inflammation, demyelination, gliosis, and axonal loss (Constantinescu, Farooqi, O'Brien, & Gran, 2011). However, the order or relation of these pathological features remains to be elucidated (Compston & Coles, 2008). Different theories have been proposed to explain how MS is triggered, but the question persists whether MS is triggered in the periphery or in the CNS (Mahad, Trapp, & Lassmann, 2015). Thus, we will further discuss this two different points of view.

The pathogenesis of MS is characterized by the development of an abnormal immune response against the CNS. Regarding the first perspective (Figure 2), this autoimmune process begins when naïve myelin-specific T cells are primed in secondary lymphoid organs (Bjelobaba, Begovic-Kupresanin, Pekovic, &

Lavrnja, 2018) by antigen presenting cells (APCs) that present myelin cross-reactive epitopes. Through an unknown mechanism, T cells become activated and undergo clonal expansion, forming a large pool of myelin-specific $CD4^+$ T cells (Bjelobaba et al., 2018). Lately, they differentiate into effector cells (Miljković & Spasojević, 2013), and start to show cross-reactivity to the myelin sheet components. To reach their target, these cells enter in the blood circulation, and ultimately enter in the CNS by crossing the main interfaces between the CNS and the periphery, the blood-brain-barrier (BBB), formed by endothelial cells, and the blood-CSF barrier, formed by the choroid plexus (Marques et al., 2012). Regarding the BBB, the crossing is accomplished upon expression of cell adhesion molecules by endothelial cells, such as intercellular adhesion molecule (ICAM)-1 and vascular cell adhesion molecule (VCAM), and via expression of their ligands by activated T cells, the integrin lymphocyte function-associated antigen (LFA)-1 and integrin very late antigen (VLA)-4, respectively (Larochelle, Alvarez, & Prat, 2011). Furthermore, the expression of active matrix metalloproteinases (MMPs), specifically MMP-2, 7 and 9, which play a role in the degradation of extracellular matrix (ECM), by T cells is required for their migration across the BBB (Larochelle et al., 2011). In addition, T cell migration through the BBB increases its permeability, which favors subsequent leukocyte infiltration (Larochelle et al., 2011). Within the CNS, effector T cells become reactivated by recognizing the myelin epitopes (Bjelobaba et al., 2018). Once reactivated, T cells will secret proinflammatory mediators, namely interferon (IFN)-γ, IL-17 and IL-6, which contributes to amplify inflammatory response through continuous activation of those cells, activation of CNS resident cells, such as microglia and astrocytes, and recruitment of other immune cells, such as B cells and mononuclear cells, from the periphery (Lassmann, Horssen, & Mahad, 2012; Mahad et al., 2015). Likewise, B cells differentiate into plasma cells upon encountering myelin epitopes (Hemmer, Archelos, & Hartung, 2002), and release large amounts of IgG, an important diagnostic marker detectable in the CSF of MS patients. The activated microglia through mechanisms including secretion of proinflammatory cytokines, and production of reactive oxygen and nitrogen species (ROS/RNS), leads to neurotoxicity and induces oligodendrocyte death (Correale et al., 2016). Overall, the combination of these events results in the formation of a lesion, characterized by apoptotic oligodendrocytes, demyelinated axons and infiltrating macrophages filled with phagocytic cell debris (Lassmann et al., 2012; Peferoen et al., 2014). In the majority of MS lesions, oligodendrocyte progenitor cells (OPCs) are recruited to the site of the lesion and differentiate into myelinating oligodendrocytes that are capable to remyelinate axons (Cao & He, 2013; Lassmann et al., 2012). Nevertheless, the mechanisms of repair in remyelination fail in MS patients, possibly due to the presence of inhibitory factors in the lesion environment (Cao & He, 2013). In some demyelinated axons, saltatory nerve-impulse conduction is replaced by continuous

conduction, through reverse operation of sodium-calcium exchanger and redistribution of sodium channels (Compston & Coles, 2008), however the nerve conduction velocity is slower than before.

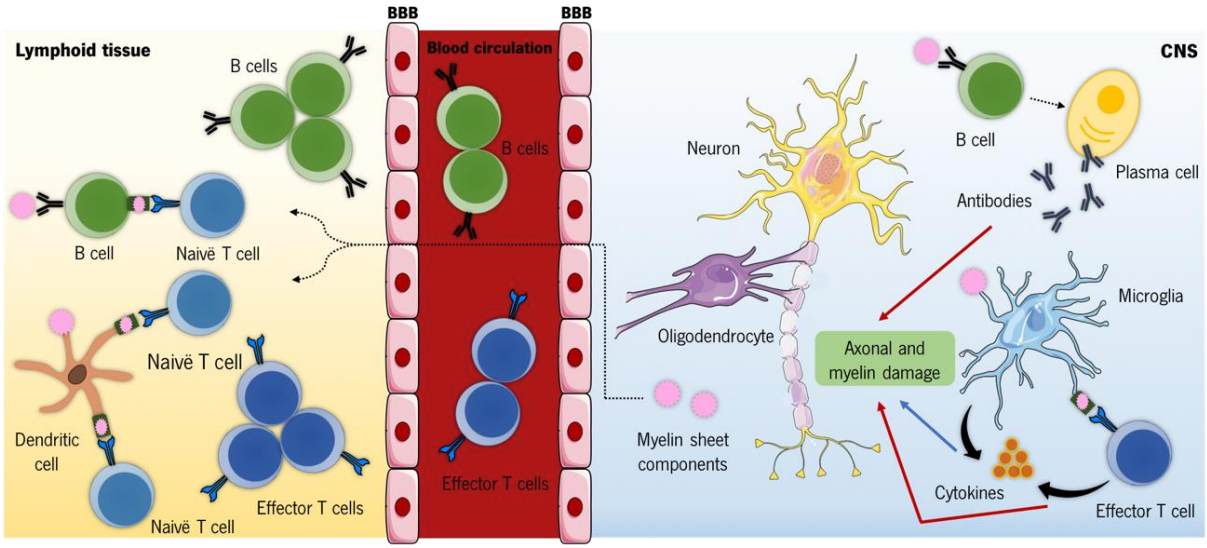

Figure 2 - Mechanisms underlying MS disease. Dendritic cells, by presenting myelin antigens that are released from the CNS, activates B and T cells in the lymphoid tissue. Once differentiated into effector cells, T cells infiltrate the CNS through the BBB by increasing its permeability, which favors subsequent leukocyte infiltration, namely B cells. Within the CNS, upon encountering myelin epitopes, T cells become reactivated and secret proinflammatory mediators, while B cells differentiate into plasma cells and release large amounts of IgG. The combination of these events results in an amplified inflammatory response, which includes the activation of CNS resident cells, such as microglia and astrocytes that also contribute to the overall CNS inflammation in MS.

Another theory for the pathogenesis of MS propose that acute damage of the CNS is the primary process, followed by neuroinflammation as a physiological mechanism for CNS protection, repair and maintenance (Sochocka, Diniz, & Leszek, 2017). Briefly, in this case, lesions result from the early loss of oligodendrocytes, leads to myelin degeneration and the activation of resident innate immune cells (Bogie, Stinissen, & Hendriks, 2014). Consequently, inflammatory mediators and other neurotoxic species are produced by these cells, causing injury to the BBB which becomes more permeable to peripheral immune cells entry (Sochocka et al., 2017). These recruited cells increase inflammatory response in the CNS by targeting the antigenic source to remove it from the CNS (Hemmer et al., 2002). It is believed that additional mechanisms are involved to explain the sustained immune response that occurs in the CNS of patients with MS, possibly alterations in the inflammatory milieu by local innate immune cells (Hemmer et al., 2002).

Overall, taking into account that the majority of MS associated genes are involved in the immunological response, the first theory that describes neurodegeneration as a consequence of immune dysregulation is favored. However, considering that MS is heterogeneous with respect to clinical, genetic, MRI and

pathological data (Popescu, Pirko, & Lucchinetti, 2013), it is highly possible that a combination of mechanisms underlies disease.

Our current knowledge on the previous MS pathological mechanisms is largely based on animal studies. Thus, in the next section, we will present the established MS animal models and discuss some of their advantages and disadvantages.

1.3. Animal models of MS

As already mentioned, the pathological mechanisms involved in MS are still poorly understood. Therefore, choosing an appropriate animal model that fully replicates the heterogeneity and complexity of MS disease is challenging. However, human studies also have limitations, such as limited access to human tissues and they only represent the end stage of the disease. Thus, the available animal models are valuable tools in MS research. Currently, there are three well-established experimental models used to study MS pathogenesis: (1) toxin-induced demyelination models; (2) virus-induced demyelination models; (3) experimental autoimmune encephalomyelitis (EAE)-induced models (Bjelobaba et al., 2018). In addition to these three models, there are also T-cell receptors (TCR) transgenic models that spontaneously develop EAE (Bjelobaba et al., 2018), and a genetic model of oligodendrocyte-induced apoptosis, applied to study the mechanism of demyelination and remyelination (Ransohoff, 2012).

Among the toxin-induced demyelination models, we are able to distinguish 2 methods to induce demyelination: direct injections of gliotoxins in the white matter tracts, such as ethidium bromide (EtBr) and lysolecithin, and systemic administration of toxins, such as cuprizone. EtBr and lysolecithin are used to create a focal demyelination lesion, and allow to predict the lesion size as well as the anatomical location (Bjelobaba et al., 2018). However, while EtBr intercalates with chromosomal deoxyribonucleic acid (DNA), being toxic for all cells with nuclei, lysolecithin targets only the myelin, leaving other cellular components relatively unaffected (Bjelobaba et al., 2018). Cuprizone is a copper chelator that causes selective toxicity for oligodendrocytes when fed to the animals, leading to demyelination in distinct brain regions, among which the corpus callosum represents the most frequently investigated (Ransohoff, 2012). This model has been highly used for gaining insights in the demyelination/remyelination process, since remyelination ensues after cuprizone withdrawal.

The virus-induced demyelination models support the hypothesis that environmental factors, such as viral infections, are involved in MS appearance and progression. The best characterized model of virus-induced demyelination is the Theiler's murine encephalomyelitis virus (TMEV). TMEV infection of susceptible

mouse strains results in the CNS autoimmune response, which comprises an early acute phase and a late chronic phase, that leads to demyelination and axonal damage (Denica et al., 2011). This is a good model to study MS pathology, since the autoimmune response that leads to axonal damage resembles MS. However, susceptible mice always develop a chronic-progressive form of disease (Denica et al., 2011), which reduces the versatility of this model.

EAE is the best characterized animal model to study MS. Since its discovery by Rivers et al. (1933), where he observed perivascular infiltrates accompanied by demyelination, in the pons and cerebellum of monkeys that were given repeated intramuscular injections of normal rabbit brain extracts, a variety of mammal species, including mice, rats, rabbits and primates have been induced with EAE (Denica et al., 2011). This model is characterized by a myelin-specific autoimmune response within the brain and spinal cord, causing demyelination and subsequent axonal injury. Therefore, due to its immunopathological and histopathological similarities with the human disease, EAE has played an important role in identifying the specific mechanisms involved in CNS inflammation and demyelination, and has been the experimental basis for many therapies tested in MS patients (Baxter, 2007; Constantinescu et al., 2011; Mecha, Carrillo-Salinas, Mestre, Feliú, & Guaza, 2013). EAE can be induced through two different approaches: actively, when animals are immunized with myelin-derived peptides, or passively, when myelin protein-specific CD4+ T cells, obtained from immunized animals or stimulated *in vitro,* are transferred into naïve animals (Constantinescu et al., 2011). In actively induced EAE, susceptible animals can be immunized with a variety of myelin-derived peptides: whole spinal cord homogenates (SCH); proteins purified from SCH, such as MBP and PLP; or myelin-specific peptides, such as MOG_{35-55} or MOG_{1-125}. Unlike MBP and PLP, that together represent around 70% of total CNS myelin proteins, MOG is a very minor component that accounts only for 0.01-0.05% of these proteins (Glatigny & Bettelli, 2018). However, MOG has emerged as an important target in MS due to its location on the surface of the oligodendrocyte cell, which makes MOG-reactive T cells more easily detected in MS patients (Glatigny & Bettelli, 2018).

The different combinations of animal species, strain, age and gender, as well as the myelin-derived peptides used, give rise to different models, that differ from each other in the type of disease course (acute monophasic, chronic progressive or relapsing-remitting), disease severity, lesion location and inflammatory environment (Constantinescu et al., 2011; Hemmer et al., 2002). The animal model chosen to study MS in the context of the present thesis was MOG_{35-55}-induced EAE mice model, specifically in C57BL/6 mice. The C57BL/6 mice induced with MOG_{35-55} present a chronic course of disease, characterized by initial tone loss in the tail, ascending to paralysis of the hind and forelimbs (Bittner, Afzali, Wiendl, & Meuth, 2014). These symptoms are resultant from the presence of multifocal, confluent

areas of mononuclear inflammatory infiltration and demyelination in the white matter of the spinal cord (Constantinescu et al., 2011). Also, in the cerebellum and hindbrain white matter, it was observed the presence of meningitis and perivascular inflammatory cuffing (Constantinescu et al., 2011). This model has been increasingly important in MS studies due to its reproducibility, and the particularity that C57BL/6 mice can be easily genetically manipulated, allowing the increased availability of gene-modified strains on this background. However, there are also some disadvantages associated. Since immunization with MOG_{35-55} alone is not sufficient to trigger disease, mice need to be induced together with a complete Freund's adjuvant (CFA), and additionally injected with pertussis toxin (PTX). CFA, usually supplemented with *Mycobacterium tuberculosis* extract, is a substance that boost the immune response through activation of the innate immune system, specifically via pattern recognition receptors (PRRs) (Awate, Babiuk, & Mutwiri, 2013). Regarding PTX, it is a significant virulence factor of Bordetella pertussis, and it is thought to facilitate immune cell entry to the CNS by increasing BBB permeability, as well as to promote proliferation and cytokine production by T cells (Bjelobaba et al., 2018; Lassmann & Bradl, 2017). This required external step is not extrapolated to MS disease, where the sensitization to myelin antigens is not artificially induced.

Furthermore, other disadvantages arise when we it comes up to all EAE models. For instance, primary demyelination that is widely seen in MS is almost absent in EAE models (Lassmann & Bradl, 2017). Instead, the mechanism of the disease starts with primary axonal injury mediated by auto-reactive CD4+ T-cells, which will lately lead to massive axonal degeneration and secondary demyelination. Also, the use of inbred strains that are kept in a specific pathogen free condition, with controlled temperature, light and humidity, does not resembles the genetic and environmental factors that are known to highly contribute to MS disease.

Altogether, there is not one single model to recapitulate all the characteristics of MS pathophysiology, but instead, a diversity of models that mimic different aspects of the disease (Figure 3). Overall, both in MS and in MS animal models there are four key pathological features of the disease: inflammation, demyelination, gliosis and axonal loss (Constantinescu et al., 2011).

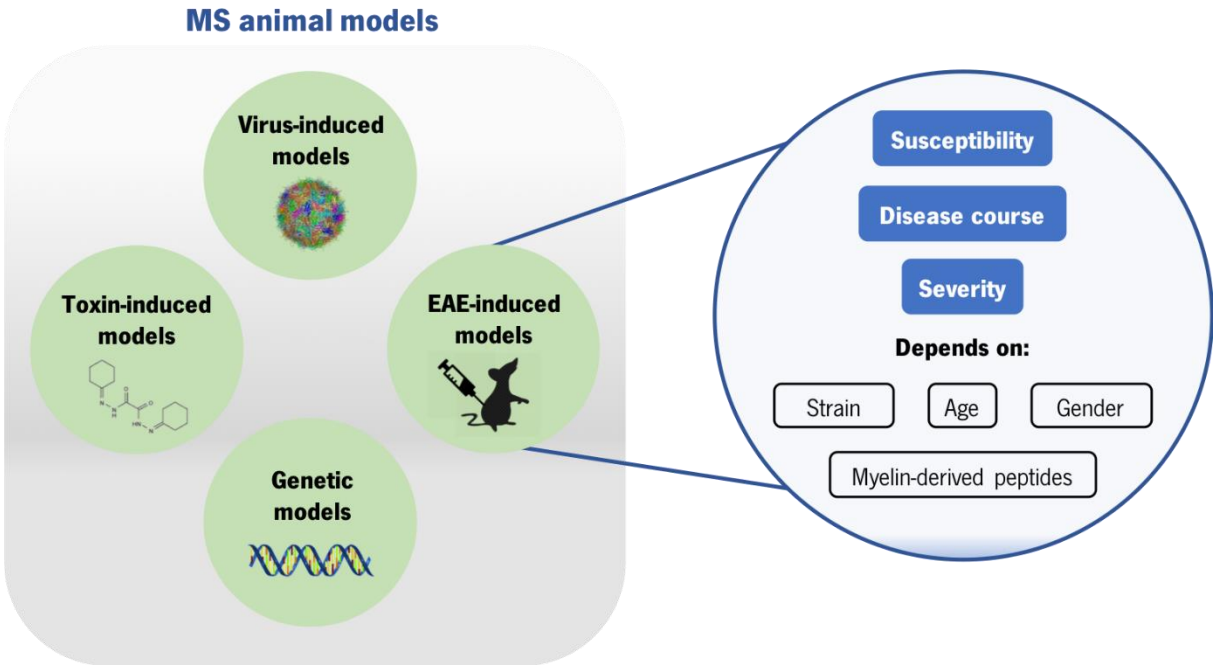

Figure 3 – Animal models of MS disease. The experimental models available to study MS pathogenesis can be subdivided into four different categories: virus-induced, toxin-induced, EAE-induced and genetic models. EAE is the most studied and applied means of studying MS, given its histopathologic similarities with disease. Besides, opposing to what happens in MS, EAE models have to be immunized with self-antigen to develop the disease. Consequently, depending on the myelin-derived peptides used, and on animal strain, age and gender, different disease susceptibility, severity and course could be developed.

As referred before, cells from the adaptative immune system (T and B cells) play a key role in the MS pathogenic mechanisms. However, because in this thesis we will address microglia, which may be considered a cell from innate immune system and also because innate immune system has an important role in MS disease we will next briefly refer to it.

1.4. The innate immune system

As referred before, much has been done to understand the etiology of MS, with a major focus on the role of the adaptive immune system. However, recent studies have suggested that the innate immune system also plays an important role both in the initiation and progression of MS by influencing the effector function of T and B cells (Weiner, 2008), but also possibly by their newly described capacity of immune memory.

Classically, the host immune responses were divided into innate immune response, which is rapid and non-specific, and adaptive immune response, which is slower to develop but highly specific due to gene rearrangements (Netea et al., 2016). Hence, one of the most powerful features of adaptive immunity is

the ability to "remember" the first encounter with a pathogen, and develop an enhanced immune response upon a second exposure (classical immunological memory) (Haley, Brough, Quintin, & Allan, 2017). During the past few years, these characteristic was only attributed to the cells of the adaptive immune system (T and B cells) however, recent findings in the immunology field introduced the concept that innate immune cells (monocytes, macrophages, DCs and NK cells) are also capable of retaining memory (a phenomenon termed as innate immune memory or trained immunity) (Netea, Quintin, & Van Der Meer, 2011; Töpfer, Boraschi, & Italiani, 2015).

The first evidence that innate immune system has the capacity to build memory came from studies in plants and invertebrates, both lacking an adaptive immune system (Arts, Joosten, & Netea, 2016; Gourbal et al., 2018; Netea et al., 2011). It was described that these organisms have the capacity to respond more efficiently to re-stimulation, both to the same or different stimulus, which emphasize the non-specificity of the innate immune system. This characteristic gave the advantage of protecting against a wide variety of stimulus, and not only the same of the first exposure (Italiani & Boraschi, 2017). This occurs because different pathogens activate the same PRRs, and because different PRRs have the same downstream signaling pathways (Crisan, Netea, & Joosten, 2016; A. P. Salam, Borsini, & Zunszain, 2017). These findings raise the question whether innate memory characteristics could also be found in vertebrates. Several experimental studies in mice came to prove that vertebrate innate immunity also share memory characteristics. For instance, it was shown that mice immunized with Bacillus Calmette-Guérin (BCG) displayed an enhanced response against infection with non-tuberculous organisms, such as *Candida albicans* (A. P. Salam et al., 2017).

The mechanisms responsible for mediating innate immune memory are quite distinct from those involved in the classical immunological memory. First, it involves a set of cells [myeloid cells, natural killer (NK) cells, and innate lymphoid cells (ILCs)] and germline-encoded recognition and effector molecules (e.g., PRRs, cytokines) that are different from those involved in classical immunological memory. Second, and in contrast to classical immunological memory that depends on gene rearrangement and proliferation of antigen-specific lymphocyte clones, the increased responsiveness to secondary stimulus during trained immunity is not specific for a particular pathogen and is mediated through signals impinging on transcription factors and epigenetic reprogramming. These are broadly defined as sustained changes in transcription programs through epigenetic rewiring, leading to changes in cell physiology that do not involve permanent genetic changes such as mutations and recombination. Finally, trained immunity relies on an altered functional state of innate immune cells that persists for weeks to months, rather than years, after the elimination of the initial stimulus.

Trained immunity not only involves rewiring the intracellular immune signaling of innate immune cells, but also induces profound changes in cellular metabolic pathways such as glycolysis, oxidative phosphorylation, fatty acid and amino acid metabolism (Arts et al., 2016) increasing the capacity of the innate immune cells to respond to a secondary stimulation. Processes such as a shift of glucose metabolism from oxidative phosphorylation to glycolysis resulting in more lactate production has been described (Jha et al., 2015) (Figure 4). This shift is assumed to be important as glycolysis, although being less efficient in terms of adenosine triphosphate (ATP) production can be upregulated multiple folds and therefore results in a faster production of ATP compared to oxidative phosphorylation ((Otto Warburg, Wind, & Negelein, 1927).

Other crucial pathway in this process is the tricarboxylic acid cycle (TCA) cycle, leading to oxidation of various substrates, including pyruvate coming from glycolysis. After induction of trained immunity with ß-glucan, trained macrophages display a decrease in oxygen consumption which suggest a decrease in the use of oxidative phosphorylation. However, the TCA cycle is not completely shut down, with concentrations of several metabolites in the TCA cycle such as citrate, succinate and fumarate being increased compared to non-trained macrophages. Increased citrate concentrations might serve as a source of fatty acid synthesis. Citrate can be produced in the TCA cycle both from pyruvate coming from glycolysis but, especially in the case of decreased pyruvate production, it can be derived from other metabolites such as glutamine. Importantly, the production of fatty acids from citrate includes first the production of acetyl-coenzyme A which is an acetyl donor for histone acetylation and it induces histone acetylation of genes of glycolytic enzymes such as hexokinase 2, phosphofructokinase and lactate dehydrogenase therefore promoting glycolysis. In addition, succinate and fumarate have been shown to play an important role in inflammation ((Mills & O'Neill, 2014). Both were described to have a stabilizing effect on hypoxia inducible factor (HIF)-1α and thus lead to an increase in glycolysis.

The understanding of these intracellular processes opens new therapeutic possibilities for the modulation of the innate immune responses during infections and inflammatory diseases. This is, indeed a very new interesting field – the immunometabolism that has gained more interest in the last several years, and has been shown to be involved in immune activation in several diseases such as infections (Palmer et al., 2016; Shi, Eugenin, & Subbian, 2016), autoinflammatory disorders and cardiovascular disease (Christ, Bekkering, Latz, & Riksen, 2016).

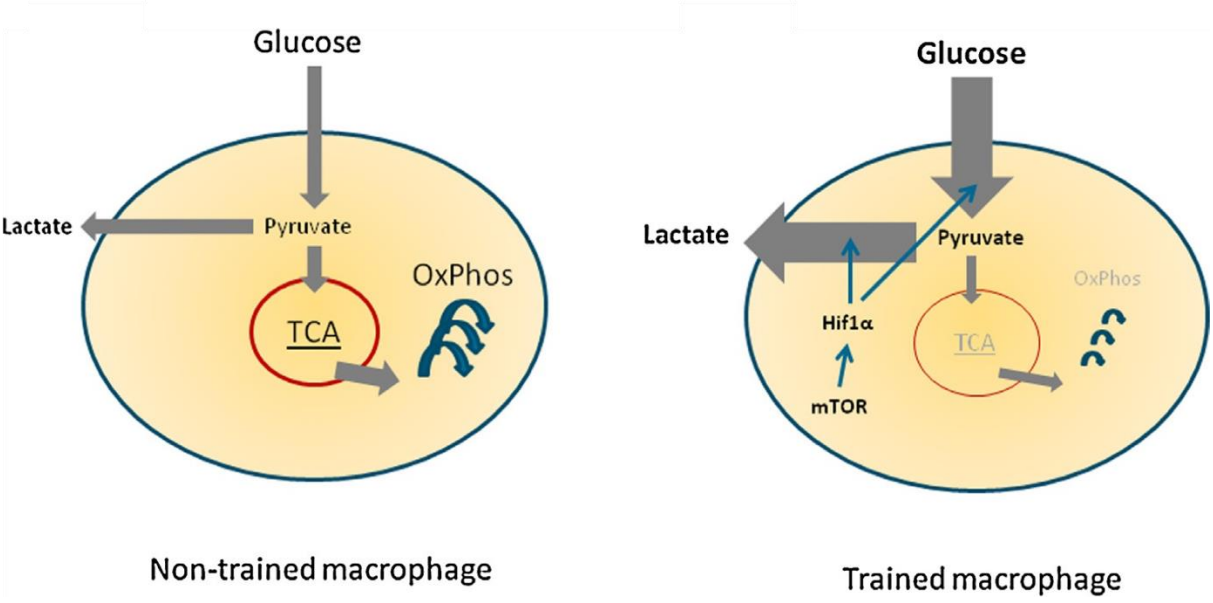

Figure 4 – Glucose metabolism in trained immunity. After induction of trained immunity with ß-glucan, trained macrophages activate the mTOR pathway and, consequently, up-regulates Hif-1α, a transcription factor of glycolysis-related genes. This results in a glucose metabolism shift from oxidative phosphorylation towards glycolysis. Pyruvate, the end product of glycolysis, is converted into lactate rather than be used as fuel to the TCA cycle, which feds energy to oxidative phosphorylation (Adapted from Arts, Joosten & Netea, 2016).

Indeed, the molecular bases of enhanced activation of a subset of inflammatory genes in trained immunity are only partially defined, but evidence show that changes in chromatin organization and the persistence of micro ribonucleic acids (RNAs) induced by the primary stimulus may be involved (Seeley et al., 2018) (Seeley et al., 2018). In terms of epigenetics, as referred above, cells modify their histone methylation and acetylation, leading to gene transcriptional changes upon subsequent stimulation (Dominguez-Andres & Netea, 2018). These changes cause long-term alterations in innate immune cells, increasing their capacity to respond to a secondary stimulus. A recent study showed that both lipopolysaccharide (LPS) and ß-glucan induce trained immunity through a mitogen-activated protein kinase (MAPK)–dependent pathway that phosphorylates the transcription factor ATF7, subsequently reducing the repressive histone mark H3K9me2 (Yoshida et al., 2015). Also, as referred before, a critical metabolic intermediate that is increased in trained monocytes (acetyl–coenzyme A) is required for histone acetylation which leads to epigenetic modifications. Additionally, the ratio of the Krebs cycle metabolites α-ketoglutarate and succinate is a critical determinant for the activity of two families of enzymes controlling epigenetic modifications: the jumonji (JMJ) family of lysine demethylases and the ten-eleven translocation (TET) family of methyl-cytosine hydroxylases (Saeed et al., 2014). These enzymes require α-ketoglutarate as a cofactor, whereas succinate limits their activity. An additional possibility for innate immune memory may be that stimulation of macrophages causes an elevation in the level of succinate; this would then inhibit

JMJD3, leading to enhanced H3K27 trimethylation of particular genes (e.g., those associated with the M2 phenotype), thus suppressing their expression (Carey, Finley, Cross, Allis, & Thompson, 2015). This process would maintain a proinflammatory phenotype of trained macrophages upon re-stimulation. Important links between altered metabolites and epigenetic changes have also been demonstrated in LPS-induced tolerance, in which nicotinamide adenine dinucleotide–dependent activation of class III histone deacetylases (sirtuins) functions in coordinating a switch from glucose to fatty acid oxidation (Liu, Vachharajani, Yoza, & McCall, 2012).

In the brain, recent studies broaden a new evidence that innate immune memory is predominantly mediated by microglia and demonstrate its impact in neuropathology (Wendeln et al., 2018). Thus, in the next chapter, we will address the main characteristics of microglia, as well as their role in MS pathophysiology and in innate immune memory.

1.5. Microglia

1.5.1. Microglia in MS disease

Microglial cells represent approximately 10-20% of glial cells (Gandhi, Laroni, & Weiner, 2011), and are located in the parenchyma of the CNS (Shemer, Erny, Jung, & Prinz, 2015). These cells, unlike the other glia types, arise from primitive myeloid progenitors in the yolk sac, and migrate to the CNS during embryogenesis (Hemmer, Kerschensteiner, & Korn, 2015). Due to their myeloid origin, microglia are considered to be the tissue-resident macrophages which makes them able to circulate and migrate within different regions of the brain. In this sense, microglia are the CNS-resident innate immune cells and not only contribute to homeostasis during health, but also represent the first line of defense against exogenous and endogenous threats (Giunti, Parodi, Cordano, & De, 2014). Under homeostatic conditions, microglia display a “resting” phenotype, characterized by a ramified morphology which allows them to actively scan the surrounding environment for insults (K. K. Thompson & Tsirka, 2017). Also, microglia has an important role in the modulation of neuronal activity by removing dysfunctional synapses and promoting the formation of new ones (O’Loughlin, Madore, Lassmann, & Butovsky, 2018; K. K. Thompson & Tsirka, 2017). Upon disturbance of CNS homeostasis, the number of microglial cells increase and they adopt an “activated” phenotype, changing their morphology into an amoeboid appearance (Peferoen et al., 2014). Activated microglia developed an acute inflammatory response to repair the damaged area of the brain, by increasing their phagocytic capacity, the production of proinflammatory mediators and neurotoxic molecules, as well as the expression of markers associated with antigen presentation which are at low

levels during homeostasis (Labzin, Heneka, & Latz, 2018; Zrzavy et al., 2017). In a normal condition, this inflammatory response is self-limited and reveals to be neuroprotective (Sochocka et al., 2017). However, under chronic inflammatory reactions, microglia activation is related with overproduction of proinflammatory mediators which can override the beneficial effects of these cells (Sochocka et al., 2017).

Recent progress in understanding MS and its animal model suggests major roles for microglia in the disease, which have drastically changed our view on the function of microglia in MS. In this context microglia are present during early and late stages of disease, and accumulate at the sites of active demyelination and neurodegeneration (O'Loughlin et al., 2018). There is good agreement that cells with a morphological microglia phenotype (small cells with elongated nuclei and ramified cell processes) dominate in initial lesion areas of new active MS lesions and at the site of lesion expansion in chronic lesions (Barnett & Prineas, 2004; Marik, Felts, Bauer, Lassmann, & Smith, 2007; Zrzavy et al., 2017), whereas cells with a macrophage phenotype populate the lesions after the initial destruction of myelin and the phagocytosis of myelin debris (Bruck et al., 1995). Because of the difficulty in distinguishing monocytes and microglia, both morphologically and functionally, the complex roles of microglia versus monocytes in the inflammatory/degenerative cascade in MS have not been fully revealed yet. However, with the advancement of specific markers and identification of molecular signatures of these cells, significant advancements are being made in this field (Butovsky et al., 2014; Rinchai, Boughorbel, Presnell, Quinn, & Chaussabel, 2016).

Recently, single-cell RNA-sequencing analysis described a disease-associated microglia (DAM) phenotype in an Alzheimer's disease (AD) mouse model, characterized by an increased expression of phagocytic-related genes and elevation of lipid metabolism pathways (Keren-Shaul et al., 2017). This DAM phenotype has been identified in other models of neurodegenerative diseases, namely in amyotrophic lateral sclerosis (ALS) and EAE, by loss of their homeostatic gene signature and up-regulation of inflammation-associated genes, suggesting a general response of microglia to CNS disturbance (Krasemann et al., 2017). The mechanisms underlying DAM phenotype are still under investigation, but studies already allowed the identification of triggering receptor expressed on myeloid cells (TREM)2-apolipoprotein E pathway as a major regulator of these transcriptional changes in neurodegenerative diseases (Krasemann et al., 2017). In fact, previous studies in EAE model showed that blockage of TREM2 with a monoclonal antibody before the appearance of the first symptoms leads to an exacerbated disease course with increased demyelination in the brain parenchyma (Piccio et al., 2007). Of interest, a single-cell mass cytometry analysis allowed the identification of three different CNS-resident myeloid populations during different EAE stages (Ajami et al., 2018). Two populations that can also be identified in the healthy CNS

(CD317^{+}MHC-II^{-}CD39^{low}CD86^{-} and CD317^{+}MHC-II^{-}CD39^{hi}CD86^{+}), and one that seems to be disease-specific (CD317^{+}MHC-II^{+}CD39^{hi}CD86^{+}). Interestingly, the disease-specific population of microglia showed an increased expression of major histocompatibility complex (MHC)-II, which is in agreement with previous studies that reported a major role for microglia in antigen presentation at early stages of EAE (Sosa, Murphey, Cardona, Ji, & Forsthuber, 2013). Additionally, the secretion of pro- and anti-inflammatory mediators by activated microglia play an important function in disease mediation. Therefore, the characterization and regulation of the signaling pathways involved in the expression of inflammatory genes is crucial to prevent chronic inflammation. A recent study identified tumor necrosis factor, alpha-induced protein 3 (*TFAIP3)* or A20 as a new anti-inflammatory protein involved in the regulation of activated microglia, with proven effects in MS (Voet et al., 2018). In that work they demonstrated that mice with A20 deficiency in microglia developed exacerbated EAE due to hyperactivation of NLRP3 inflammasome, which enhances IL-1ß secretion and CNS inflammation. Importantly they also confirmed that seems to be relevant for the human disease as they observed higher expression of A20/ *TFAIP3, NLRP3* and *IL-1ß* in plaques of MS patients. In fact, another study showed that EAE animals treated with an inhibitor of caspase-1, VX-765, presents reduced CNS inflammation by suppression of microglial inflammasome activation (McKenzie et al., 2018). Of interest, connexin 30 has recently been identified as also playing a role in EAE through microglia modulation (Fang et al., 2018). The absence of this protein showed, in chronic but not in acute EAE, the improvement of clinical symptoms and demyelination, along with an anti-inflammatory profile of microglia.

Of interest, a new role related with trained immunity by microglial cells has been described. Importantly, the modulation of this microglia immune memory, by the induction of a tolerant *versus* trained microglia phenotype can have an impact in modulation of the chronic inflammatory status associated with autoimmune disease where a decreased inflammatory response is needed which seems to be relevant in the context of MS.

1.5.2. Microglial memory: training and tolerance

Recently, similarly to macrophages, it was shown that microglia, upon an initial stimulus, is able to develop immune memory to have an enhanced immune response against future challenges (training state), or develop memory to be less reactive to future challenges (tolerance state) (Ifrim et al., 2014; Salam et al., 2017(Ifrim et al., 2014; Alex P Salam et al., 2017). The dichotomy between training and tolerance depends on several factors, such as dose and nature of the stimulus, as well as duration of the

exposure (Salam et al., 2017). A variety of stimulus was already studied in the context of innate immune memory, being LPS the most intensively described agent (Bodea et al., 2014; Ellestad et al., 2009; Püntener, Booth, Perry, & Teeling, 2012).

LPS, also known as an endotoxin, is a major component of the cell wall in most Gram-negative bacteria, and is recognized by toll-like receptor (TLR)4 (Morris, Gilliam, & Li, 2014). Wendeln et al. (2018) described that different LPS peripheral paradigms can trigger either immune training, promoting neuropathology, or immune tolerance, alleviating neuropathology, in microglia, which was confirmed in models of AD and stroke. In this work, the goal was to test whether the training- and tolerance-inducing stimulus (1X LPS and 4X LPS, respectively) has an impact in AD and stroke disease outcome. Strikingly, immune training (1X LPS) in an AD mouse model, exacerbates cerebral amyloid beta load, whereas immune tolerance (4X LPS) decreases both plaque load and total amyloid beta levels. Interestingly, peripheral immune stimulation also modulates pathological outcomes after stroke, strongly reducing the volume of neuronal damage and microglial activation in immune tolerant animals (4X LPS) (Wendeln et al., 2018). Of note, and contrary to previous work in infection models, both studies are concordant and seem to suggest that, at least in CNS disease models, training promotes, while tolerance alleviates pathology. Nevertheless, both states are mediated through epigenetic and metabolic reprogramming. In terms of epigenetic reprogramming, training and tolerance phenotypes are associated with histone modifications, such as acetylation at lysine 27 of histone 3 (H3K27ac) and tri-methylation at lysine 4 of histone 3 (H3K4me3) (Dominguez-Andres & Netea, 2018). Upon pathogen exposure, cells modify their histone acetylation and methylation, affecting their gene expression patterns in response to a second stimulation. Regarding metabolic reprogramming, the induction of a training state in microglia leads to a shift from oxidative phosphorylation towards aerobic glycolysis (Dominguez-Andres & Netea, 2018; Netea, Latz, Mills, & Neill, 2015). As referred, this mechanism is used to rapidly produce energy, and ultimately to generate metabolites with immunomodulatory functions, such as fumarate and succinate, that play an important function in the long-term reprogramming of these cells (Dominguez-Andres & Netea, 2018).

Altogether, linking the concept of innate immune memory with microglia profile in the CNS, it become reasonable to study the possible benefits of this association in disease such as MS where a predominant inflammatory component should be tackled. Thus, knowing that inflammation in the periphery can prompt immune responses in the brain, we intent to use different LPS paradigms as stimulators (1 and 4 LPS injections) in the EAE mouse model.

1.6. Research objectives

Focused on the brain-resident macrophages (microglia), we hypothesized that modulation of these cells towards immune tolerance could promote neuroprotection and reduce disease burden. Therefore, to determine whether the training- (1X LPS) and tolerance-induced (4X LPS) peripheral stimulus could lead to long-term alterations in brain immune responses and thereby modify MS pathogenesis, we will take advantage of the EAE model in a C57BL/6 background. Also, we will specifically study the cerebellum, which is a region commonly affected in MS disease. Specifically, we aim to understand the impact of peripheral immune stimulation on the CNS of EAE mice, at the onset and chronic phases of disease, by analyzing clinical disease score, demyelinating lesions, astrocytic morphology and the expression level of inflammatory cytokines and glial activation markers.

2. Materials and Methods

2.1. Animals

Animal handling and experimental procedures were conducted in accordance with the Portuguese national authority for animal experimentation, *Direção Geral de Alimentação e Veterinaária* (ID: DGAV9458). Animals were kept in accordance with the guidelines for the care and handling of laboratory animals in the Directive 2010/63/EU of the European Parliament and the Council. Also, experiments were performed taking the 3Rs principles (Replacement, Reduction and Refinement) in consideration. The animals were housed and maintained in a controlled environment at 22-24°C and 55% humidity, on 12 hour light/dark cycles (lights on at 8 a.m.) and fed with regular rodent's chow and tap water *ad libitum*.

2.2. Peripheral immune stimulation

In an attempt to understand if the training- and tolerance-induced stimulus could have an impact on the CNS of EAE mice, we injected the animals with different LPS paradigms. For that, 60 two-month-old female mice were randomly assigned to treatment groups (Figure 5A), and were injected intraperitoneally (i.p.) with LPS (L6511; Sigma-Aldrich®, Saint Louis, MO, USA) at a daily dose of 500 μg per kg of bodyweight. Animals received either four LPS injections on four consecutive days (4X LPS), or a single LPS injection followed by three vehicle injections on the following three days (1X LPS) or four vehicle injections (Saline) (Figure 5B).

2.3. Induction and clinical evaluation of EAE

One month after the last LPS injection, 10 animals from each group were induced with EAE, and other 10 animals were used as controls (non-induced) (Figure 5A). EAE was induced in the animals with the Hooke Kit™ MOG_{35-55}/CFA Emulsion PTX (EK-2110; Hooke Laboratories, Lawrence, MA, USA). For that, animals were immunized subcutaneously at the lower and upper back, with an emulsion of MOG_{35-55} in CFA (1:1), followed by an i.p. administration of PTX in phosphate buffer solution (PBS), after 2 and 24 hours of immunization (100 ng of PTX per injection). Non-induced animals received an emulsion of PBS in CFA (1:1) (non-induced) (CK-2110; Hooke Laboratories), and were injected i.p. with PTX in PBS (Figure 5B).

A. Experimental groups

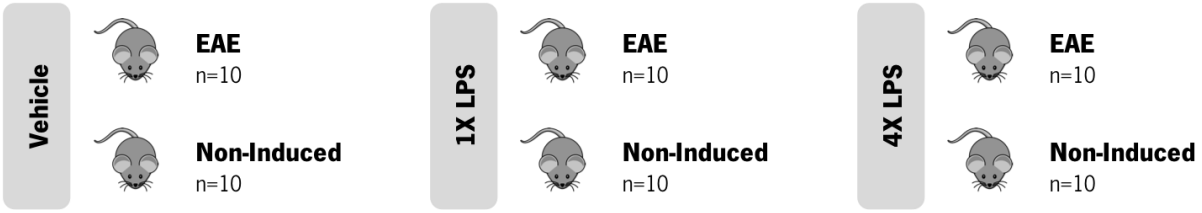

B. Experimental timeline

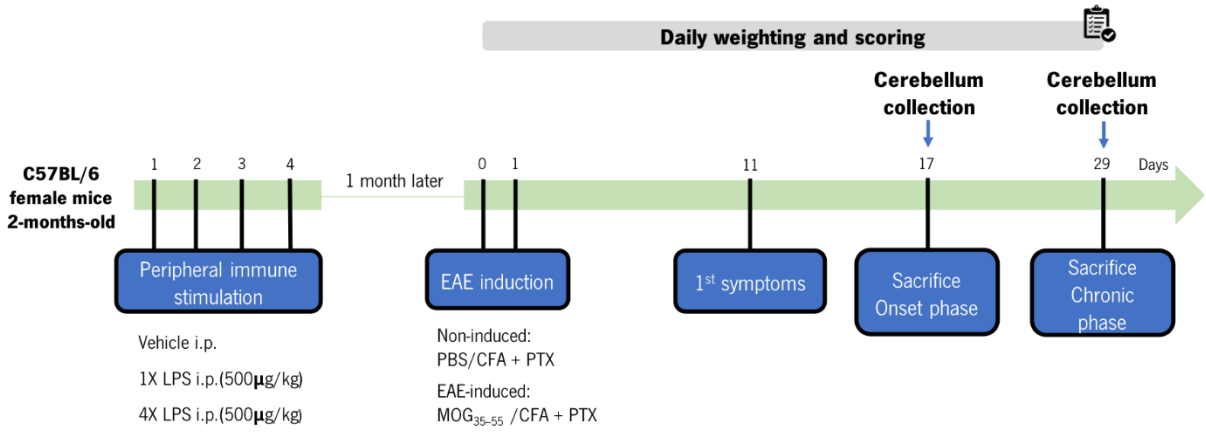

Figure 5 – Scheme of the experimental design of peripheral stimulation with LPS paradigms and EAE induction. A group of 60 C57BL/6 females was equally randomly assigned to three different treatment groups, after which 10 animals of each group were induced with EAE, and the other 10 animals were used as controls (A). Regarding treatment with LPS, animals received either four LPS injections on four consecutive days (4X LPS), or a single LPS injection followed by three vehicle injections on the following three days (1X LPS) or four vehicle injections (Saline). One-month later, EAE was induced. The first symptoms appeared at day 11 post-EAE induction, and we collect the cerebellum from animals at day 17 (onset phase) and at day 29 (chronic phase) for further analysis. Animals were monitored daily for the progression of disease and weight measurements (B).

After immunization, animals were weighted and examined daily in order to monitor the appearance of EAE clinical signs. Disease severity was evaluated according to the scoring guidelines in Table 1. To avoid bias in scoring, mice were scored in a blinded way.

Table 1 - Mouse EAE scoring guidelines.

Score	Clinical Observations
0.0	No obvious changes in motor function compared to non-immunized mice
0.5	Partially limp tail
1.0	Paralyzed tail
1.5	At least one of the hind legs falls through consistently when the animal is dropped on a wire rack
2.0	Loss of coordinated movement, wobbly walk
2.5	Dragging of the hind limbs
3.0	Complete paralysis of both hind legs
3.5	Hind limbs paralyzed and weakness in forelimbs
4.0	Complete hind limbs and partial forelimbs paralysis
4.5	Animal is not alert, no movement
5.0	Moribund state or found dead due to paralysis

2.4. Tissue sample collection and storage

At the onset (day 17 post-EAE induction) and chronic (day 29 post-EAE induction) phases of disease, animals were anesthetized with an i.p. injection of ketamine hydrochloride (150 mg/kg, Imalgene® 1000) plus medetomidine hydrochloride (0.3 mg/kg, Dorben®). Under deep anesthesia, mice were transcardially perfused with cold 0.9% saline solution. For gene expression analysis, brains were macrodissected under conventional light stereomicroscope, and cerebellum region was snap-frozen and stored at -80°C. For histological analysis, brains were immediately embedded in Tissue-tek® O.C.T™ compound (4583; Sakura, Alphen aan den Rijn, Netherlands), snap-frozen and kept frozen at -20°C until further sectioning.

2.5. Luxol Fast Blue staining

The histochemical staining Luxol Fast Blue was used to assess the lesioned areas, with inflammatory infiltrates, in the cerebellum' white matter. For that, brains embedded in Tissue-tek® O.C.T™ compound

were sectioned at 20 μm (coronal sections) in the cryostat, and cerebellum sections were fixated in 95% ethanol at room-temperature (RT) for 15 minutes, followed by the overnight incubation, at 55-56°C, with 0.5% Luxol Fast Blue MBS (HD1575-25; TCS Biosciences, Botolph Claydon, Buckingham, UK). On the day after, the excess of solution was removed firstly with 95% ethanol, and then with running tap water. The tissue was differentiated with 0.05% lithium carbonate (62470; Sigma-Aldrich®) for 10 minutes, and with 70% ethanol for 1 minute. After counterstaining with hematoxylin, slides were dehydrated and mounted with Entellan® (107961; Merck Millipore, Burlington, Massachusetts, USA).

The quantification of the total lesioned area was performed in 8 non-consecutive representative sections of the cerebellum. Sections were visualized with an Olympus Stereological Microscope (Olympus, Hamburg, Germany), and the quantification of lesion areas of animals euthanized at the onset phase was performed with the Visiopharm® image analysis software platform (Visiopharm, Hoersholm, Denmark), while the quantification of lesion areas of animals euthanized at the chronic phase was performed with the Stereo Investigator software (MBF Bioscience, Williston, Vermont, US). The total white matter area was drawn using an objective of 4x, and the lesion areas were delimitated using an objective of 10x. The percentage of lesioned area was calculated by dividing the sum of the lesioned areas by the total white matter area.

2.6. Gene expression analysis by qRT-PCR

Gene expression levels were determined using quantitative real-time Polymerase Chain Reaction (qRT-PCR) approach. Total RNA was isolated from the cerebellum using TRIzol® Reagent (15596018; Invitrogen, Thermo Fisher Scientific). Briefly, 1 mL of TRIzol® was added to the frozen tissue, which was mechanically disrupted using a 20G needle. Samples were incubated for 5 minutes at RT, after which 200 μL of chloroform (C2432; Sigma-Aldrich®) were added and the samples were mixed vigorously. Samples were incubated for 3 minutes at RT and centrifuged for 15 minutes at 8000 rpm, 4°C. After centrifugation, 3 phases were visible: an upper aqueous phase, which contains the RNA, an interphase, which contains the DNA, and a lower red phenol-chloroform phase, which contains cells debris and proteins. To precipitate the RNA, the upper phase was transferred into a new eppendorf tube, and 500 μL of isopropanol were added. Samples were incubated for 10 minutes at RT, and centrifuged for 10 minutes at 9000 rpm, 4°C. To eliminate the isopropanol, the RNA pellet was washed with 75% ethanol, and samples were centrifuged for 7 minutes at 6000 rpm, 4°C. The RNA pellet was resuspended in 20

μL of sterile water, and RNA quantification was performed using the NanoDrop® (Thermo Scientific, Thermo Fisher Scientific) spectrophotometer, diluting the samples to a final concentration of approximately 1 μg/μL.

To remove contaminating DNA, 4 μg of RNA was treated with DNase I (EN0525; Thermo Scientific, Thermo Fisher Scientific). Briefly, the RNA was transferred to a new RNase free tube, together with 1U/μg RNA of DNase I, 1 μL 10x reaction buffer with $MgCl_2$ and nuclease-free water until a final volume of 10 μL. Samples were incubated at 37°C for 30 minutes. After adding 1 μL of 50 mM ethylenediamine tetraacetic acid (EDTA), samples were placed in the pre-heated block at 65°C for 10 minutes, and then transferred to ice until RNA quantification in the NanoDrop®.

The reverse transcription of 1 μg of RNA from each sample into complementary DNA (cDNA) was performed using the iScript™ cDNA Synthesis Kit (170-8891; Bio-Rad Laboratories, Hercules, California, US). Briefly, 1 μg of RNA from all samples was transferred to a polymerase chain reaction (PCR) tube, plus 4 μL of 5x iScript reaction mix, 1 μL iScript reverse transcriptase and nuclease-free water to a total volume of 20 μL. The reverse transcription reaction occurred in a thermocycler (Eppendorf, Hamburg, Germany), according to the conditions presented in Table 2.

Table 2 - Mix and reaction conditions used for cDNA synthesis.

PCR reagent	Volume (μL)	PCR conditions
RNA	Corresponding to 1 μg of RNA	5 minutes at 25°C
5x iScript reaction mix	4	30 minutes at 42°C
iScript reverse transcriptase	1	5 minutes at 85°C
Nuclease-free water	Until a final volume of 20	∞4°C

The qRT-PCR of samples from animals sacrificed at the onset phase of disease was carried on Applied Biosystems™ 7500 Fast Real-Time PCR System (Fisher scientific, Thermo Fisher Scientific), with the commercial kit 5x HOT FIREPol® EvaGreen® qPCR Mix Plus (08-24-00020; Solis BioDyne, Tartu, Estonia), according to the manufacturer's program instructions (Table 3). Briefly, a mix was prepared for each

sample with 14 μL of nuclease-free water, 0.5 μL of 10 μM forward and reverse primers and 4 μL of 5x HOT FIREPol® EvaGreen® qPCR Mix Plus. Then, 1 μL of cDNA was added to each PCR tube.

Table 3 - Reaction conditions used for qRT-PCR with the commercial kit 5x HOT FIREPol® EvaGreen® qPCR Mix Plus.

Reaction step	Temperature (ºC)	Time (seconds)	Number of cycles
Initial activation	95	720	1
Denaturation	95	15	40
Annealing	Primer specific	20	
Elongation	72	20	

The qRT-PCR of samples from animals sacrificed at the chronic phase of disease was carried on a CFX96™ Real-Time System (Bio-Rad Laboratories), with the commercial kit SsoFast™ EvaGreen® Supermixes (172-5201; Bio-Rad Laboratories), according to the manufacturer's instructions (Table 4). Briefly, a mix was prepared for each sample with 3 μL of nuclease-free water, 0.5 μL of 10 μM forward and reverse primers and 5 μL of SsoFast™ EvaGreen® Supermix. Then, 1 μL of cDNA was added to each PCR tube.

Table 4 - Reaction conditions used for qRT-PCR with the commercial kit SsoFast™ EvaGreen® Supermixes.

Reaction step	Temperature (ºC)	Time (seconds)	Number of cycles
Enzyme activation	95	900	1
Denaturation	95	15	39
Annealing	Primer specific	20	
Extension	72	20	
Melting curve	65 to 95	5	1

The fluorescence of the PCR product was detected at the end of the elongation cycle. All melting curves exhibited a single sharp peak at the expected temperature. The reference genes ATP synthase F1 subunit

beta mitochondrial (*Atp5b*) and heat shock 90kD protein 1 beta (*Hspcb*) were used as internal standards for the normalization of the expression of selected transcripts. The sequence and respective annealing temperatures of the selected transcripts are presented in Annex 1.

2.7. Immunofluorescence and 3D morphometric analysis of astrocytes

To assess the morphology of astrocytes in the cerebellum' white matter, frozen sections of the cerebellum were stained for glial fibrillary acidic protein (GFAP), which is a marker for astrocytes and whose expression is highly correlated to astrocytic morphological alterations. The staining protocol started with a fixation step in which sections of the cerebellum were immersed in paraformaldehyde (PFA) 4% at RT for 30 minutes, followed by three washes with PBS. Immediately after antigen retrieval step, with pre-heated citrate buffer 10mM (C9999; Sigma-Aldrich®) in the microwave for 20 minutes, tissue sections were transferred to water and washed three times with PBS-Triton 0.3% for 3 minutes each, to permeabilize the tissue. Tissue sections were blocked with fetal bovine serum (FBS) 10% in PBS-Triton 0.3% for 30 minutes at RT in humid chamber, followed by the overnight incubation, at RT, with the primary antibody rabbit anti-mouse GFAP antibody (1:200; Z033401; Dako, Glostrup, Hovedstaden, Denmark), diluted in FBS 10% PBS-Triton 0.3%. On the next morning, tissue sections were rinsed in PBS-Triton 0.3% and then incubated with the secondary antibody Alexa Fluor 594 goat anti-rabbit (1:500; A11037; Invitrogen, Thermo Fisher Scientific, Waltham, Massachusetts, US) diluted in PBS-Triton 0.3% for 2 hours at RT in humid chamber. After rinsing tissue sections with PBS-Triton 0.3%, the double-stranded DNA was labeled by 5 minutes incubation with DAPI (1:200; D1306; Invitrogen, Thermo Fisher Scientific) diluted in PBS. Finally, tissue sections were rinsed in PBS and cover-slipped with Immu-Mount (9990402; Fisher scientific, Thermo Fisher Scientific) mounting medium.

Z-stacks of confocal images were obtained using a 40x magnification objective (1024x1024 pixel resolution; stepsize of 1 μm) in an Olympus FV1000 confocal microscope (Olympus). Z-stacks were uploaded to the FIJI-Image J Simple Neurite Tracer (SNT) plugin software where we analyze a total of 6 enteric astrocytes per treatment group as previously reported (Tavares et al., 2017). Specifically, the structural features analyzed were: total process length, process arbor complexity (Sholl analysis) and process thickness. The total process length was determined by the sum of the length of individual paths reconstructed. The process arbor complexity was estimated from the number of intersections at each radial distance from the starting point provided by the "Sholl analysis" function. The process thickness was estimated from the GFAP thickness.

2.8. Statistical analysis

Statistical analysis were performed with GraphPad Prism version-7.0 (GraphPad, Inc., La Jolla, California, USA) and IBM® SPSS® Statistics Version 25.0 (IBM, Armonk, New York, USA). The study of the impact of peripheral immune stimulation in disease clinical score and weight was analyzed using a repeated measures (RM) two-way ANOVA. The mean day when animals presented the first symptoms, the mean first clinical score given to the animals, the mean maximum score that animals reached, and the mean day when animals reached a clinical score of 3 were analyzed by one-way ANOVA. The percentage of inflammatory infiltrates in the cerebellum' white matter area was also statistically compared by one-way ANOVA. The expression levels of inflammatory cytokines and genes related with the activation of glial cells were analyzed using two-way ANOVA. To compare the total length and process thickness among groups for astrocytic 3D morphologic reconstructions, a two-way ANOVA test was applied. To the Sholl analysis data for astrocyte 3D reconstruction a mixed ANOVA test was applied. Results are presented throughout as mean±standard error of the mean (SEM) and the statistical significance of the comparisons for each statistical test was set with a confidence interval of 95%.

3. Results

3.1. Chronic disease course in MOG_{35-55} EAE model is similar among LPS pretreatment groups

Upon peripheral stimulation with different LPS paradigms mice were challenged, 1 month after, with EAE as described previously. Herein our aim was to understand if the training- (1X LPS) and tolerance-induced (4X LPS) stimulus could modify the disease course. For that reason, we evaluated not only the overall disease development, but also specific EAE clinical outcomes. We performed two different experiments: in the first one we sacrificed the animals at the onset phase of the disease, and in the second one we sacrificed the animals at the chronic phase of the disease.

As expected, EAE animals developed a chronic disease course and started to lose weight around day 11 post-disease induction in both experiments, coincidently with the appearance of the first symptoms in some animals. Also, the body weight variation was similar among EAE groups during the experiment (Figure 6A, C). When analyzing overall disease development, no significant differences were found in the clinical score among EAE groups, neither in the onset experiment (first experiment) (treatment factor: $F(2,27)=1.372$, $p<0.0001$; time factor: $F(6,162)=186.4$, $p=0.2708$; interaction: $F(12,162)=1.338$, $p=0.2015$) nor in the chronic experiment (second experiment) (treatment factor: $F(2,27)=0.7546$, $p=0.4799$; time factor: $F(18,486)=60.63$, $p<0.0001$; interaction: $F(36,486)=0.9592$, $p=0.5394$), as shown in Figure 6B and 6D, respectively.

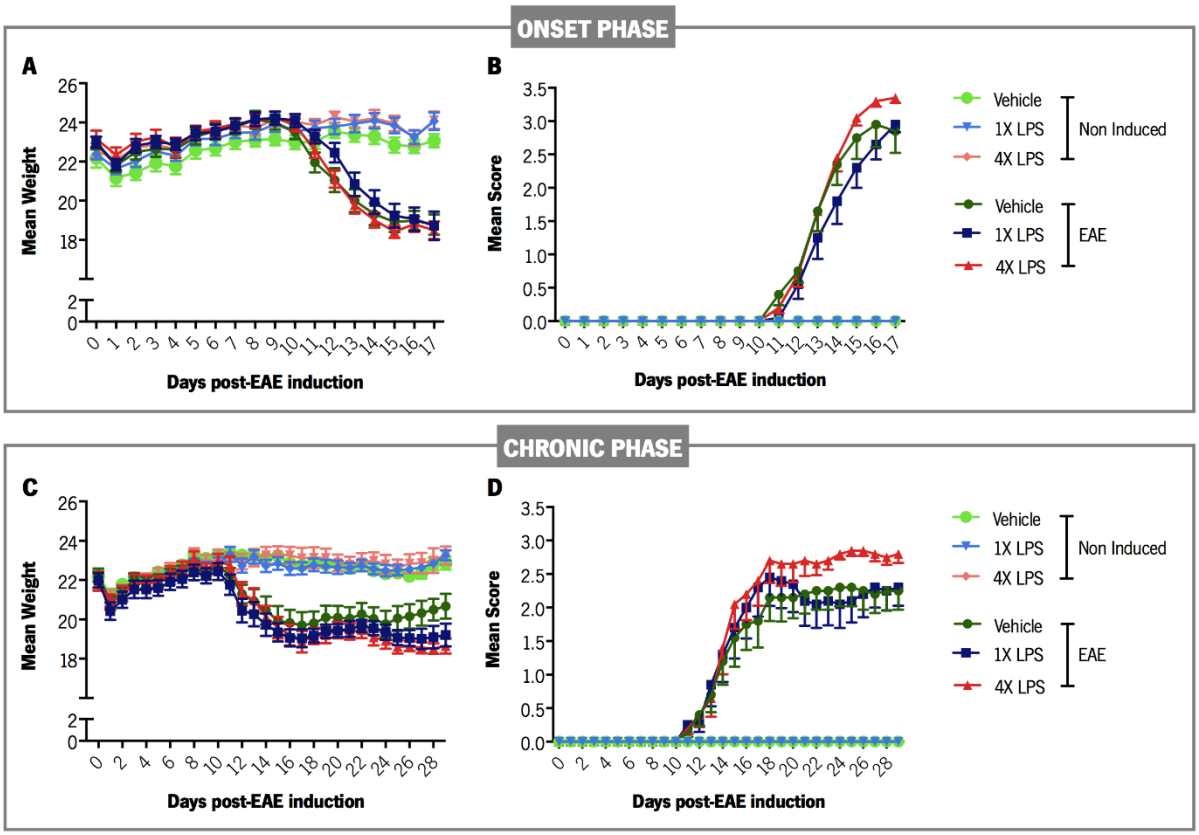

Figure 6 - Disease course of MOG_{35-55}-induced EAE animals upon peripheral stimulation with different LPS paradigms. In the first experiment, EAE animals started to lose weight at around day 11, coincidently with the appearance of the first symptoms in some animals (A), and reached the peak of disease at around day 17 (onset phase of the disease) (B). In the second experiment, EAE animals started to lose weight also at around day 11 (C), and after reaching the peak of disease, the animals remained with a similar score until the end of the experiment, at day 29 (chronic phase of the disease) ($n_{Vehicle\text{-}non\text{-}induced}$ = 10, $n_{1XLPS\text{-}non\text{-}induced}$ = 10, $n_{4XLPS\text{-}non\text{-}induced}$ = 10, $n_{Vehicle\text{-}EAE}$ = 10, $n_{1XLPS\text{-}EAE}$ = 10, $n_{4XLPS\text{-}EAE}$ = 10).

Regarding specific-disease measures, EAE animals exposed to a training-induced stimulus (1X LPS) and sacrificed at the onset phase of disease presented a significant delay in the appearance of the first symptoms when compared to EAE control animals, which was not observed in the experiment where EAE animals were sacrificed at the chronic phase of disease (Table 5). Other specific disease measurements were also analyzed, such as the mean first clinical score given to the animals, the mean maximum score that animals reached, and the mean day when animals reached a clinical score of 3, however no differences were observed among the EAE animals neither in the onset experiment nor in the chronic experiment. Regarding disease incidence, one animal of the vehicle group from the onset experiment did not develop disease symptoms, as well as one animal of the vehicle group and one animal of the 1X LPS group from the chronic experiment. Even though, we did not exclude none of those animals from the analysis since they exhibited infiltration of inflammatory cells in the cerebellum' white matter.

Table 5 – EAE clinical outcomes in different LPS pretreatment groups at the onset and chronic phases of disease.

		Disease incidence	Day of first symptoms (n)	First clinical score (higher than 0) (n)	Maximum score (n)	Day of clinical score=3 (n)
Onset phase	Vehicle	9/10	11,56±0,24 (9)	0,61±0,07 (9)	2,95±0,34 (10)	3,44±0,29 (9)
	1X LPS	10/10	12,70±0,40 (10)	0,75±0,17 (10)	2,95±0,12 (10)	4,56±0,41 (9)
	4X LPS	10/10	11,90±0,28 (10)	0,60±0,10 (10)	3,35±0,08 (10)	3,60±0,31 (10)
	F-test value		3,422	0,4578	1,203	3,066
	p value		0,0479	0,6377	0,3160	0,0644
Chronic phase	Vehicle	9/10	13,11±0,75 (9)	0,45±0,05 (9)	2,40±0,31 (10)	6,75±2,78 (4)
	1X LPS	9/10	14,22±1,48 (9)	0,55±0,09 (9)	2,75±0,34 (10)	3,43±0,20 (7)
	4X LPS	10/10	13,00±0,73 (10)	0,80±0,20 (10)	3,05±0,14 (10)	3,25±0,16 (8)
	F-test value		0,4173	1,929	1,411	3,083
	p value		0,6635	0,1649	0,2613	0,0737

3.2. EAE animals exposed to a training-induced stimulus exhibit increased infiltration of inflammatory cells at the chronic phase of disease but not at the onset phase

Although most studies using the EAE animal model are focused especially on spinal cord lesions, the cerebellum has been shown to be highly affected in this model. For this reason, we sought to characterize the cerebellar inflammatory area of EAE animals after peripheral stimulation with LPS paradigms, by quantifying the percentage of inflammatory infiltrates in the white matter. We chose to study these effects in a more active phase of disease (onset phase) and at the chronic phase of the disease. To evaluate these lesioned areas, we stained representative sections of the whole cerebellum with the histochemical coloration Luxol Fast Blue. As shown in Figure 7A and 7C, hematoxylin revealed clusters of infiltrating cells in the cerebellum of EAE mice in each pretreatment condition at both disease time points, and an absence of these inflammatory cell infiltrates in the cerebellum of non-induced mice. To obtain a measurement of the percentage of lesioned area, we sum all the areas where we found these clusters and divided by the total white matter area. At the onset phase of disease, no significant differences were observed in the percentage of lesioned area among LPS pretreatment groups (EAE Vehicle=14.2±3.421,

EAE 1X LPS=11.54±7.083, EAE 4X LPS=9.385±6.248; F(2,9)=0.5126, p=0.6154) (Figure 7B). Regarding the chronic phase of disease, EAE animals that were exposed to a training-induced stimulus (1X LPS) presented a higher percentage of lesioned area, in the cerebellar white matter, when compared to EAE animals exposed to a tolerance-induced stimulus (4X LPS) and also when compared to EAE control animals (EAE Vehicle=6.749±0.934, EAE 1X LPS=19.39±4.13 , EAE 4X LPS=5.32±2.09; F(2,9)=8.064, p=0.0098) (Figure 7D).

These results might suggest that immune training profile, elicited by 1X LPS paradigm, display an enhanced immune response against EAE, but only in a later phase of the disease (chronic phase).

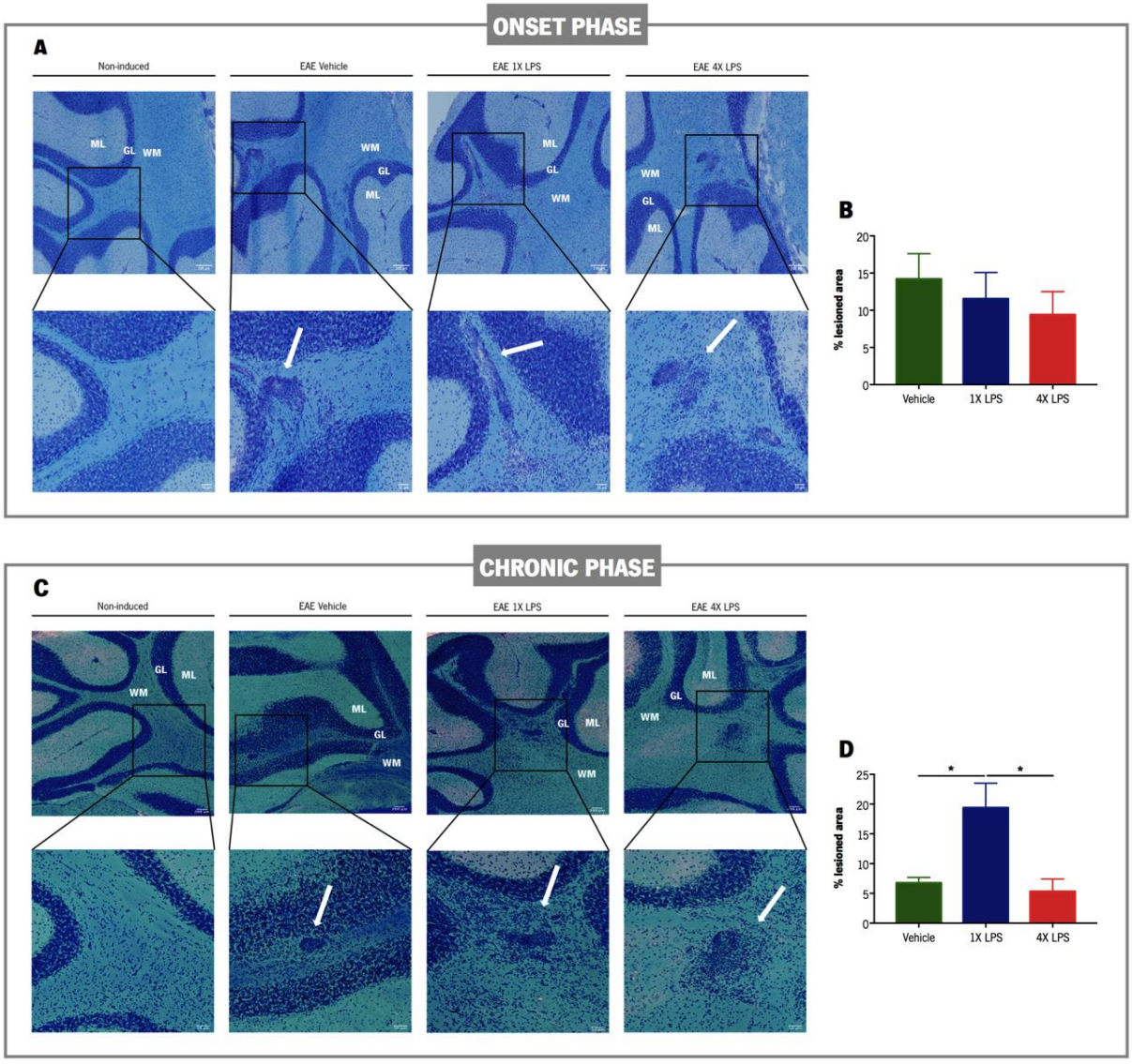

Figure 7 - Luxol Fast Blue staining for myelin in EAE cerebellum sections at the onset and chronic phases of the disease. The cerebellar white matter of animals induced with EAE present lesioned areas that are absent in non-induced mice. These lesioned areas are identified after luxol fast blue staining as areas with clusters of inflammatory infiltrates (arrows) (upper panel bar = 200 μm, lower panel bar = 50 μm) at the onset phase (A) and at the chronic phase of the disease (C). The percentage of lesioned area was obtained by the sum of all the areas where we found these clusters, divided by the total white matter area, for the animals sacrificed at the onset

phase of disease (B) and for the animals sacrificed at the chronic phase of the disease (D) ($n_{Vehicle\text{-}EAE}$ = 4, $n_{1XLPS\text{-}EAE}$ = 4, n_{4XLPS} = 4. WM – white matter; ML – molecular layer; GL – granular layer). *p<0.05.

3.3. Distinct gene expression profiles of inflammatory cytokines at the onset phase of the disease *versus* the chronic phase

For the gene expression analysis, we selected genes mainly involved in T helper (Th)1 and Th17 immune responses, which are the cells that predominantly mediates EAE lesions (Domingues, Mues, Lassmann, Wekerle, & Krishnamoorthy, 2010). Regarding the cytokines involved in Th1 immune response, namely *Ifn-gamma* (Figure 8A, F) and *Il-12* (Figure 8B, G), were both increased in the cerebellum of EAE animals during the onset phase of the disease but, during the chronic phase, only the expression levels of *Ifn-gamma* were significantly increased. When analyzing the expression levels of *Il-17* (Figure 8C, H), a cytokine involved in Th17 immune response, a significant increase was observed in the cerebellum of EAE animals at both disease time points. We also decided to evaluate the expression levels of a cytokine involved in Th2 immune response, *Il-4* (Figure 8D, I) which are decreased in the EAE animals when compared to the non-induced during the onset phase of the disease, and not altered during the chronic phase of the disease. Of interest, considering these four genes, no differences were observed when the LPS pretreatment groups are compared. The expression levels of *Il-6* (Figure 8E, J), a multifunctional cytokine that is described as a promotor of EAE clinical manifestations (Samoilova, Horton, Hilliard, Liu, & Chen, 1998), were observed to be significantly increased in the EAE animals when compared to the non-induced in the two disease time points. Specifically, at the onset phase of the disease, *Il-6* was significantly more expressed in EAE animals exposed to a training-induced stimulus (1X LPS) when compared to EAE animals exposed to a tolerance-induced stimulus (4X LPS) and also when compared to EAE control animals.

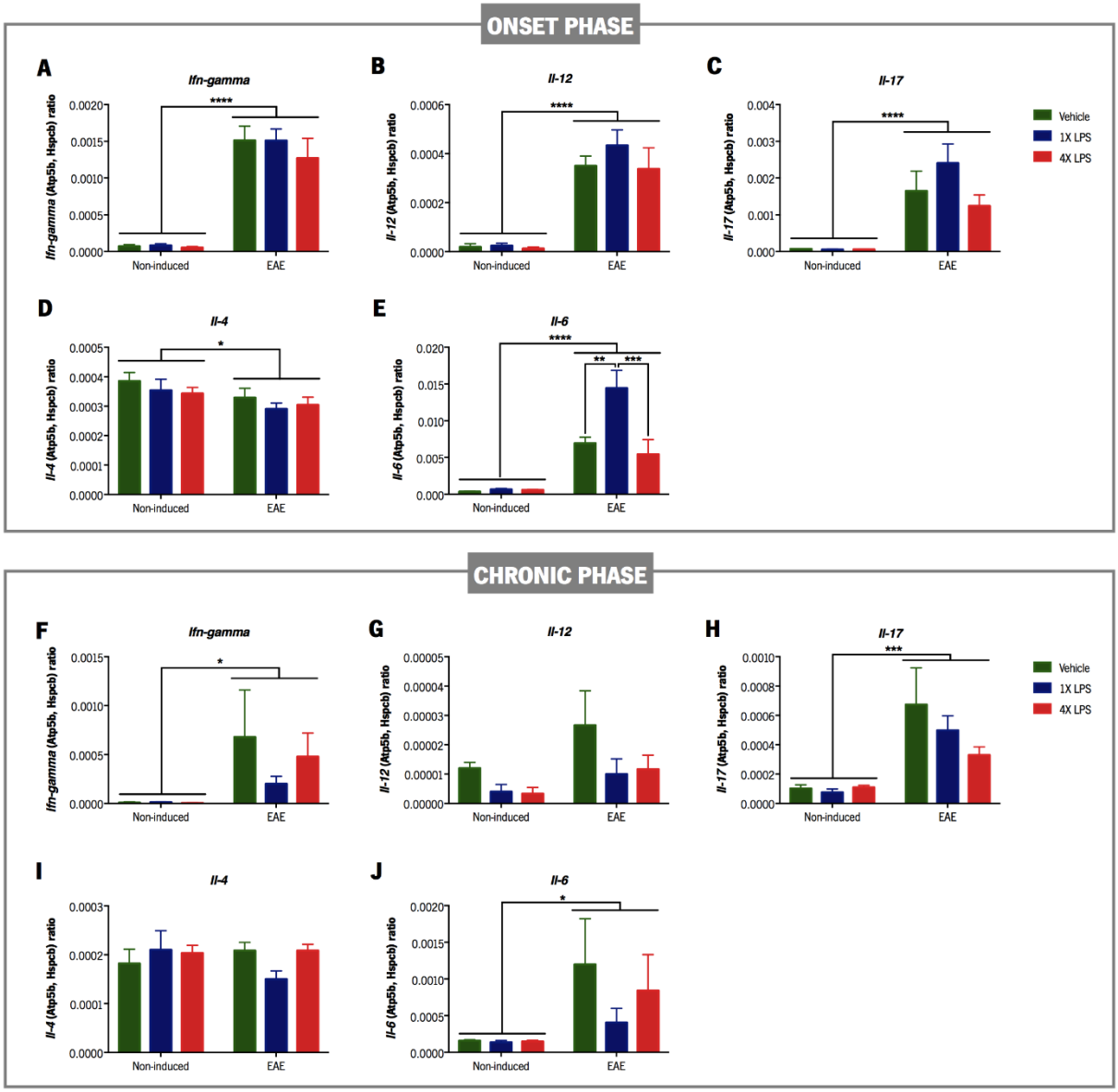

Figure 8 - Expression levels of inflammatory cytokines in the cerebellum of EAE animals at the onset and chronic phases of the disease. Gene expression levels of *Ifn-gamma* (A, F) and *Il-12* (B, G), cytokines involved in Th1 immune response, *Il-17* (C, H), a cytokine involved in Th17 immune response, *Il-4 (D, I),* a cytokine involved in Th2 immune response, and *Il-6 (E, J)*, a multifunctional cytokine that is described as a promotor of EAE clinical manifestations, were assessed by qRT-PCR at the onset and chronic phases of the disease. All samples were normalized to *Atp5b* and *Hspcb*. (onset, $n_{Vehicle\text{-}non\text{-}induced} = 6$, $n_{1XLPS\text{-}non\text{-}induced} = 6$, $n_{4XLPS\text{-}non\text{-}induced} = 6$, $n_{Vehicle\text{-}EAE} = 6$, $n_{1XLPS\text{-}EAE} = 6$, $n_{4XLPS\text{-}EAE} = 6$; chronic, $n_{Vehicle\text{-}non\text{-}induced} = 5$, $n_{1XLPS\text{-}non\text{-}induced} = 5$, $n_{4XLPS\text{-}non\text{-}induced} = 6$, $n_{Vehicle\text{-}EAE} = 6$, $n_{1XLPS\text{-}EAE} = 6$, $n_{4XLPS\text{-}EAE} = 6$). *p<0.05, **p<0.01, ***p<0.001, ****p<0.0001.

The results of two-way ANOVA analysis for the onset and chronic phases of the disease are presented in table 6 and table 7, respectively.

Table 6 – Two-way ANOVA results of the gene expression analysis of inflammatory cytokines in the cerebellum at the onset phase of the disease.

			Mean±SEM	Disease factor	Treatment factor	Interaction
Ifn-gamma	**Vehicle**	Non-induced	7.17e-5±2.46e-5	F (1,30) = 122, p < 0.0001	F (2,30) = 0.5062, p = 0.6078	F (2,30) = 0.3435, p = 0.7120
		EAE onset	1.51e-3±1.93e-4			
	1X LPS	Non-induced	8.17e-5±2.37e-5			
		EAE onset	1.51e-3±1.58e-4			
	4X LPS	Non-induced	5.33e-5±1.41e-5			
		EAE onset	1.27e-3±2.71e-4			
Il-12	**Vehicle**	Non-induced	1.90e-5±1.33e-5	F (1,30) = 85.54, p < 0.0001	F (2,30) = 0.7443, p = 0.4837	F (2,30) = 0.5006, p = 0.6111
		EAE onset	3.51e-4±3.93e-5			
	1X LPS	Non-induced	2.42e-5±1.02e-5			
		EAE onset	4.34e-4±6.29e-5			
	4X LPS	Non-induced	1.27e-5±6.25e-6			
		EAE onset	3.38e-4±8.63e-5			
Il-17	**Vehicle**	Non-induced	7.33e-5±6.67e-6	F (1,30) = 39.86, p < 0.0001	F (2,30) = 1.579, p = 0.2228	F (2,30) = 1.618, p = 0.2151
		EAE onset	1.65e-3±5.41e-4			
	1X LPS	Non-induced	5.17e-5±1.05e-5			
		EAE onset	2.41e-3±5.23e-4			
	4X LPS	Non-induced	5.50e-5±5.63e-6			
		EAE onset	1.24e-3±2.99e-4			
Il-4	**Vehicle**	Non-induced	3.86e-4±2.93e-5	F (1,30) = 5.144, p = 0.0307	F (2,30) = 0.9774, p = 0.3879	F (2,30) = 0.09525, p = 0.9094
		EAE onset	3.29e-4±3.17e-5			
	1X LPS	Non-induced	3.54e-4±3.83e-5			
		EAE onset	2.91e-4±1.95e-5			
	4X LPS	Non-induced	3.43e-4±2.06e-5			
		EAE onset	3.04e-4±2.67e-5			
Il-6	**Vehicle**	Non-induced	3.42e-4±7.94e-5	F (1,30) = 60.73, p < 0.0001	F (2,30) = 6.937, p = 0.0033	F (2,30) = 6.409, p = 0.0048
		EAE onset	6.94e-3±8.18e-4			
	1X LPS	Non-induced	6.55e-4±1.15e-4			
		EAE onset*	1.44e-2±2.41e-3			
	4X LPS	Non-induced	5.70e-4±7.90e-5			
		EAE onset	5.43e-3±2.00e-3			

Table 7 - Two-way ANOVA results of the gene expression analysis of inflammatory cytokines in the cerebellum at the chronic phase of the disease.

			Mean±SEM	Disease factor	Treatment factor	Interaction
Ifn-gamma	Vehicle	Non-induced	8.00e-6±8.00e-6	F (1,28) = 5.239, p < 0.05	F (2,28) = 0.4854, p = 0.6205	F (2,28) = 0.505, p = 0.6089
		EAE chronic	6.78e-4±4.82e-4			
	1X LPS	Non-induced	1.20e-5±3.74e-6			
		EAE chronic	2.00e-4±7.70e-5			
	4X LPS	Non-induced	3.33e-6±3.33e-6			
		EAE chronic	4.78e-4±2.42e-4			
Il-12	Vehicle	Non-induced	1.20e-5±2.00e-6	F (1,28) = 3.1 p = 0.0643	F (2,28) = 2.537, p = 0.0971	F (2,28) = 0.2592, p = 0.7735
		EAE chronic	2.67e-5±1.17e-5			
	1X LPS	Non-induced	4.00e-6±2.45e-6			
		EAE chronic	1.00e-5±5.16e-6			
	4X LPS	Non-induced	3.33e-6±2.11e-6			
		EAE chronic	1.17e-5±4.77e-6			
Il-17	Vehicle	Non-induced	1.02e-4±2.44e-5	F (1,28) = 16.79, p < 0.001	F (2,28) = 0.9837, p = 0.3865	F (2,28) = 1.086, p = 0.3515
		EAE chronic	6.73e-4±2.51e-4			
	1X LPS	Non-induced	7.60e-5±2.25e-5			
		EAE chronic	4.98e-4±9.91e-5			
	4X LPS	Non-induced	1.10e-4±1.29e-5			
		EAE chronic	3.30e-4±5.61e-5			
Il-4	Vehicle	Non-induced	1.82e-4±2.92e-5	F (1,28) = 0.2795, p = 0.6012	F (2,28) = 0.6953, p = 0.5073	F (2,28) = 2.011, p = 0.1527
		EAE chronic	2.08e-4±1.68e-5			
	1X LPS	Non-induced	2.10e-4±3.91e-5			
		EAE chronic	1.50e-4±1.67e-5			
	4X LPS	Non-induced	2.03e-4±1.58e-5			
		EAE chronic	2.08e-4±1.30e-5			
Il-6	Vehicle	Non-induced	1.58e-4±1.28e-5	F (1,28) = 5.253, p < 0.05	F (2,28) = 0.6352, p = 0.5373	F (2,28) = 0.5688, p = 0.5726
		EAE chronic	1.20e-3±6.23e-4			
	1X LPS	Non-induced	1.36e-4±2.54e-5			
		EAE chronic	4.05e-4±1.93e-4			
	4X LPS	Non-induced	1.47e-4±1.93e-5			
		EAE chronic	8.40e-4±4.92e-4			

3.4. Glial cells are activated in the cerebellum of EAE mice both at the onset and chronic phases of the disease

One of the key pathological features of MS and EAE is the activation of glial cells, namely astrocytes and microglia. To evaluate the astrocytic and microglial response to peripheral stimulation with different LPS paradigms in the cerebellum of EAE animals, we performed qRT-PCR for specific gene transcripts related

with the activation of these cells in the two disease time points. When analyzing the genes related to astrocyte activation, either the levels of *Gfap* (Figure 9A, G) and lipocalin 2 *(Lcn2)* (Figure 9B, H) were increased in the EAE animals when compared to the non-induced at both disease time points. Also, during the onset phase of the disease, the expression levels of *Gfap* were significantly increased in the EAE animals exposed to a training-induced stimulus (1X LPS) when compared to the animals exposed to a tolerance-induced stimulus (4X LPS) and also when compared to EAE control animals. When genes related to microglia activation were analyzed, an increased expression of ionized calcium-binding adapter molecule 1 *(Iba1)* (Figure 9C, I), CX3C chemokine receptor 1 *(Cx3cr1)* (Figure 9D, J) and *Mhc-II* (Figure 9E, K) was observed in the EAE animals compared to the non-induced at both disease time points, while the expression levels of inducible nitric oxide synthase *(inos)* (Figure 9F, L) were only significantly increased in the EAE animals during the onset phase of the disease. Nevertheless, no differences were observed when the LPS pretreatment groups are compared. The results of two-way ANOVA analysis for the onset and chronic phases of the disease are presented in table 8 and table 9, respectively.

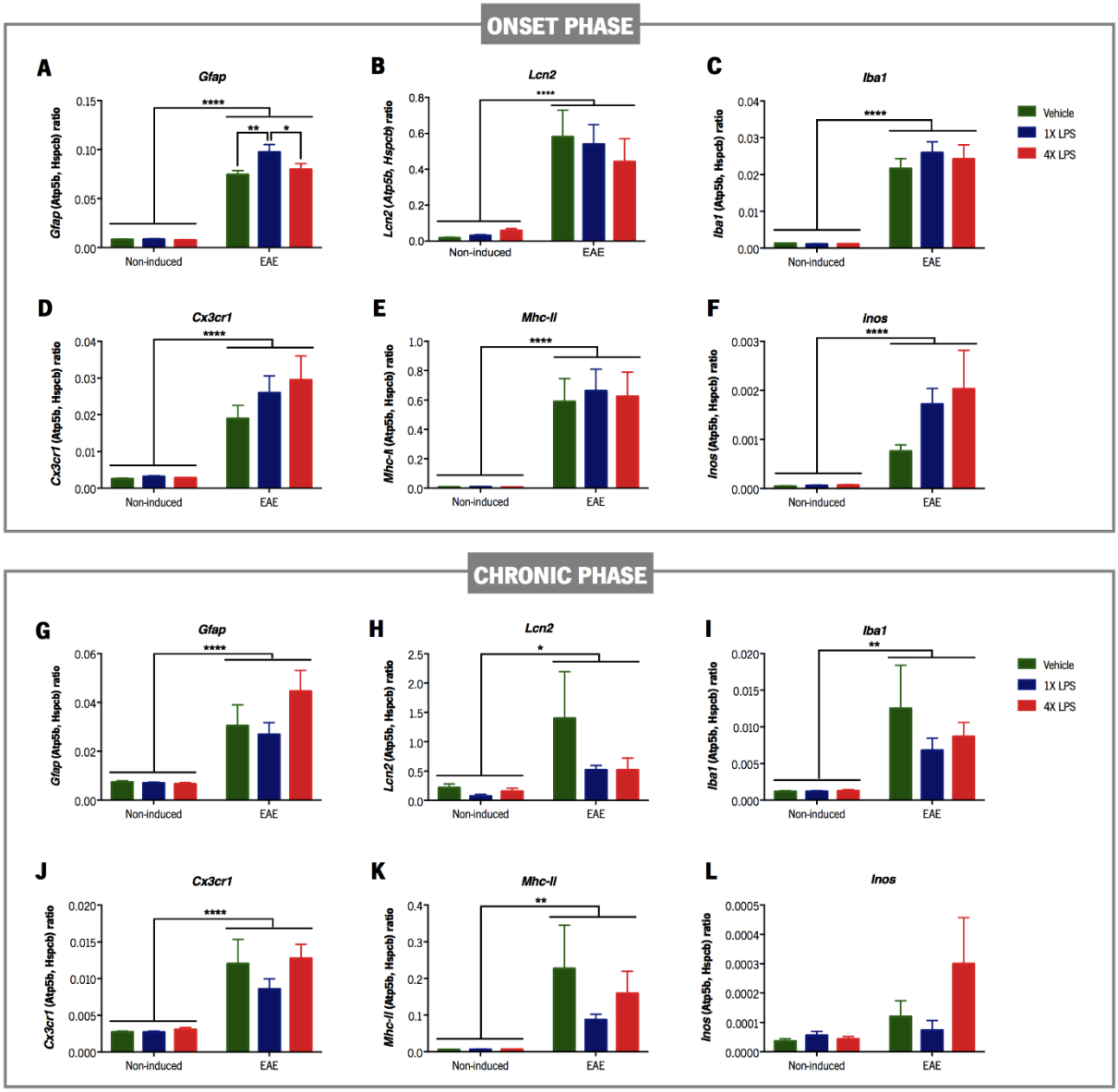

Figure 9 - Expression levels of genes related with the activation of astrocytes and microglia in the cerebellum of EAE animals at the onset and chronic phases of disease. Gene expression levels of *Gfap* (A, G) and *Lcn2* (B, H), which are markers related to the activation of astrocytes, and *Iba1* (C, I), *Cx3cr1* (D, J), *Mhc-II* (E, K) and *inos* (F, L), which are markers related to the activation of microglia, were assessed by qRT-PCR at the onset and chronic phases of the disease. All samples were normalized to *Atp5b* and *Hspcb*. (onset, $n_{Vehicle\text{-}non\text{-}induced} = 6$, $n_{1XLPS\text{-}non\text{-}induced} = 6$, $n_{4XLPS\text{-}non\text{-}induced} = 6$, $n_{Vehicle\text{-}EAE} = 6$, $n_{1XLPS\text{-}EAE} = 6$, $n_{4XLPS\text{-}EAE} = 6$; chronic, $n_{Vehicle\text{-}non\text{-}induced} = 5$, $n_{1XLPS\text{-}non\text{-}induced} = 5$, $n_{4XLPS\text{-}non\text{-}induced} = 6$, $n_{Vehicle\text{-}EAE} = 6$, $n_{1XLPS\text{-}EAE} = 6$, $n_{4XLPS\text{-}EAE} = 6$). *p<0.05, **p<0.01, ***p<0.001, ****p<0.0001.

Table 8 - Two-way ANOVA results of the gene expression analysis of markers related with the activation of astrocytes and microglia in the cerebellum at the onset phase of the disease.

			Mean±SEM	Disease factor	Treatment factor	Interaction
Gfap	**Vehicle**	Non-induced	8.23e-3±3.00e-4	F (1,30) = 452.8, p < 0.0001	F (2,30) = 3.982, p = 0.0293	F (2,30) = 3.661, p = 0.0378
		EAE onset	7.45e-2±4.20e-3			
	1X LPS	Non-induced	8.47e-3±5.96e-4			
		EAE onset*	9.75e-2±7.75e-3			
	4X LPS	Non-induced	7.53e-3±5.56e-4			
		EAE onset	7.97e-2±5.98e-3			
Lcn2	**Vehicle**	Non-induced	5.90e-2±1.13e-2	F (1,30) = 42.13, p < 0.0001	F (2,30) = 0.1484, p = 0.8627	F (2,30) = 0.5063, p = 0.6078
		EAE onset	4.43e-1±1.27e-1			
	1X LPS	Non-induced	3.12e-2±6.09e-2			
		EAE onset	5.40e-1±1.08e-1			
	4X LPS	Non-induced	1.75e-2±4.28e-3			
		EAE onset	5.81e-1±1.49e-1			
Iba1	**Vehicle**	Non-induced	1.30e-3±8.56e-5	F (1,30) = 148.9, p < 0.0001	F (2,30) = 0.4114, p = 0.6664	F (2,30) = 0.4893, p = 0.6179
		EAE onset	2.16e-2±2.67e-3			
	1X LPS	Non-induced	1.12e-3±1.66e-4			
		EAE onset	2.59e-2±2.94e-3			
	4X LPS	Non-induced	1.17e-3±1.15e-4			
		EAE onset	8.42e-2±3.93e-3			
Cx3cr1	**Vehicle**	Non-induced	2.57e-3±1.43e-4	F (1,30) = 56.09, p < 0.0001	F (2,30) = 1.191, p = 0.3179	F (2,30) = 1.036, p = 0.3671
		EAE onset	1.90e-2±3.58e-3			
	1X LPS	Non-induced	3.22e-3±1.85e-4			
		EAE onset	2.60e-2±4.63e-3			
	4X LPS	Non-induced	2.83e-3±6.67e-5			
		EAE onset	2.95e-2±6.55e-3			
Mhc-II	**Vehicle**	Non-induced	8.33e-3±6.15e-4	F (1,30) = 46.76, p < 0.0001	F (2,30) = 0.05438, p = 0.9472	F (2,30) = 0.05226, p = 0.9492
		EAE onset	5.90e-1±1.56e-1			
	1X LPS	Non-induced	9.00e-3±1.84e-3			
		EAE onset	6.62e-1±1.47e-1			
	4X LPS	Non-induced	7.00e-3±6.32e-4			
		EAE onset	6.24e-1±1.65e-1			
inos	**Vehicle**	Non-induced	4.50e-5±9.92e-6	F (1,30) = 25.59, p < 0.0001	F (2,30) = 1.859, p = 0.1734	F (2,30) = 1.729, p = 0.1947
		EAE onset	7.60e-4±1.31e-4			
	1X LPS	Non-induced	6.17e-5±9.46e-6			
		EAE onset	1.72e-3±3.22e-4			
	4X LPS	Non-induced	6.83e-5±1.28e-5			
		EAE onset	2.03e-3±7.84e-4			

Table 9 - Two-way ANOVA results of the gene expression analysis of markers related with the activation of astrocytes and microglia in the cerebellum at the chronic phase of the disease.

			Mean±SEM	Disease factor	Treatment factor	Interaction
Gfap	**Vehicle**	Non-induced	7.44e-3±5.06e-4	F (1,28) = 33.83, p < 0.0001	F (2,28) = 1.31, p = 0.2858	F (2,28) = 1.499, p = 0.2406
		EAE chronic	3.05e-2±8.52e-3			
	1X LPS	Non-induced	7.06e-3±3.58e-4			
		EAE chronic	2.69e-2±4.85e-3			
	4X LPS	Non-induced	6.63e-3±6.31e-4			
		EAE chronic	4.46e-2±8.50e-3			
Lcn2	**Vehicle**	Non-induced	2.18e-1±6.48e-2	F (1,28) = 5.073, p < 0.05	F (2,28) = 1.221, p = 0.3102	F (2,28) = 0.7704, p = 0.4724
		EAE chronic	1.40e0±7.94e-1			
	1X LPS	Non-induced	7.27e-2±3.30e-2			
		EAE chronic	5.20e-1±7.68e-2			
	4X LPS	Non-induced	1.56e-1±5.49e-2			
		EAE chronic	5.19e-1±2.04e-1			
Iba1	**Vehicle**	Non-induced	1.18e-3±1.37e-4	F (1,28) = 12.64, p < 0.01	F (2,28) = 0.5217, p = 0.5992	F (2,28) = 0.5323, p = 0.5931
		EAE chronic	1.25e-2±5.88e-3			
	1X LPS	Non-induced	1.19e-3±1.30e-4			
		EAE chronic	6.81e-3±1.66e-3			
	4X LPS	Non-induced	1.28e-3±1.73e-4			
		EAE chronic	8.68e-3±1.91e-3			
Cx3cr1	**Vehicle**	Non-induced	2.71e-3±1.38e-4	F (1,28) = 32.29, p < 0.0001	F (2,28) = 0.8619, p = 0.4333	F (2,28) = 0.6806, p = 0.5145
		EAE chronic	1.20e-2±3.33e-3			
	1X LPS	Non-induced	2.71e-3±1.47e-4			
		EAE chronic	8.59e-3±1.38e-3			
	4X LPS	Non-induced	3.05e-3±2.95e-4			
		EAE chronic	1.27e-2±1.94e-3			
Mhc-II	**Vehicle**	Non-induced	5.81e-3±3.06e-4	F (1,28) = 10.15, p < 0.01	F (2,28) = 0.6947, p = 0.5076	F (2,28) = 0.703, p = 0.5036
		EAE chronic	2.27e-1±1.18e-1			
	1X LPS	Non-induced	6.23e-3±1.50e-3			
		EAE chronic	8.72e-2±1.52e-2			
	4X LPS	Non-induced	6.49e-3±7.44e-4			
		EAE chronic	1.59e-1±6.02e-2			
inos	**Vehicle**	Non-induced	3.60e-5±8.12e-6	F (1,28) = 3.866, p = 0.0593	F (2,28) = 1.269, p = 0.2967	F (2,28) = 1.419, p = 0.2589
		EAE chronic	1.20e-4±5.37e-5			
	1X LPS	Non-induced	5.60e-5±1.36e-5			
		EAE chronic	7.33e-5±3.33e-5			
	4X LPS	Non-induced	4.33e-±8.82e-6			
		EAE chronic	3.00e-4±1.57e-4			

3.5. Astrogliosis is similarly increased in the cerebellum of EAE animals among LPS pretreatment groups during the chronic phase of the disease

Several studies described the impact of astrocytes in MS and EAE immunopathology by highlighting their morphological and structure alterations (Brambilla, 2019). For that reason, next, we investigated the impact that peripheral stimulation paradigms could have on the morphology of astrocytes. To do so, we stained cerebellum sections for GFAP, and assessed specific structural features of astrocytes in the normal appearing white matter (NAWM) and lesion areas of EAE animals, and also in the white matter of non-induced animals, both at the onset and chronic phases of the disease. Regarding the onset phase results, representative images of the GFAP staining are presented in Figure 10A. As observed in Figure 10B, and from two-way ANOVA analysis (table 10), there is a significant decrease in the total length of astrocytes in all 1X LPS groups (non-induced+lesion+NAWM) and in all 4X LPS groups (non-induced+lesion+NAWM) when compared to all vehicle groups. Regarding the process thickness (Figure 10C) analysis, no differences were observed between EAE and non-induced animals, neither among the LPS pretreatment conditions. The arbor complexity of GFAP+ astrocytes (within-subject effects - radius: $F_{GG}(3.769,101.768)=1016.068$, $p<0.0001$, radius*treatment: $F_{GG}(7.538,101.768)=7.423$, $p<0.0001$, radius*disease: $F_{GG}(7.538,101.768)=1.194$, $p=0.312$, radius*treatment*disease: $F_{GG}(15.077,101.768)=1.133$, $p=0.337$; between-subject effects – treatment: $F(2,27)=14.427$, $p<0.0001$, disease: $F(2,27=0.743$, $p=0.485$, treatment*disease: $F(4,27=)1.024$, $p=0.413$) (Figure 10D), provided by the sholl analysis, showed a decreased number of intersections at each radial distance in all 1X LPS groups (non-induced+lesion+NAWM) and in all 4X LPS groups (non-induced+lesion+NAWM) when compared to all vehicle groups (non-induced+lesion+NAWM).

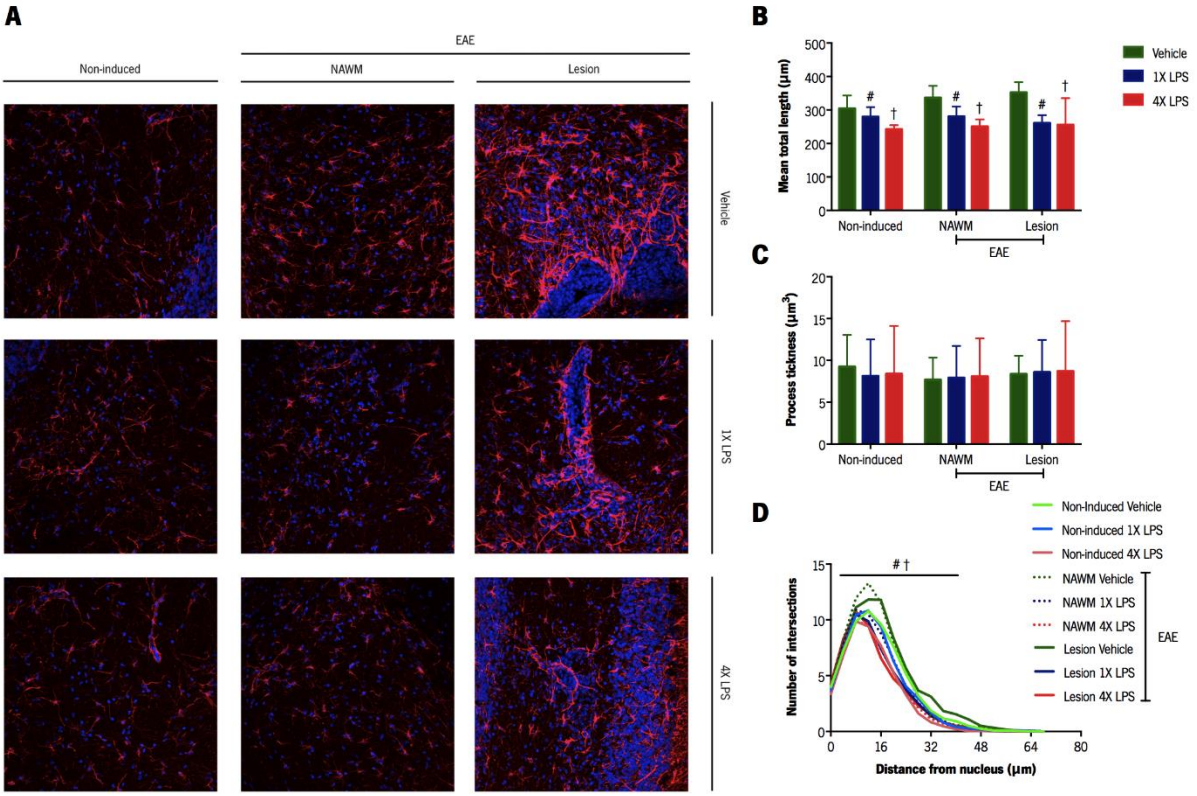

Figure 10 - GFAP immunohistochemical staining and morphological structure of astrocytes in the cerebellum at the onset phase of the disease. Representative images from the cerebellum' white matter show the presence of astrogliosis in EAE animals (A). Characterization of the 3D structure of astrocytes by analysis of total length (B), process thickness (C) and sholl intersections (D) (Each animal corresponds to the mean of 6 astrocytes). # - Statistical differences between all 1X LPS groups (non-induced+lesion+NAWM) *versus* all vehicle groups (non-induced+lesion+NAWM), $p<0.01$; † - Statistical differences between all 4X LPS groups (non-induced+lesion+NAWM) *versus* all vehicle groups (non-induced+lesion+NAWM), $p<0.0001$.

Table 10 - Two-way ANOVA results of the total length and process thickness analysis of astrocytes in the cerebellum at the onset phase of the disease.

			Mean±SEM	Disease factor	Treatment factor	Interaction
Total length	Vehicle	Non-induced	304.6±19.57	F (2,27) = 0.5411, p = 0.5883	F (2,27) = 14.56, p < 0.0001	F (4,27) = 0.7788, p = 0.5488
		NAWM	336.4±17.92			
		Lesion	352.3±15.44			
	1X LPS	Non-induced	279.6±14.37			
		NAWM	281.0±14.77			
		Lesion	261.1±11.64			
	4X LPS	Non-induced	242.3±6.195			
		NAWM	250.3±10.91			
		Lesion	255.6±39.99			
Process thickness	Vehicle	Non-induced	9.255±1.900	F (2,27) = 0.1019, p = 0.9035	F (2,27) = 0.009289, p = 0.9035	F (2,28) = 0.040039, p = 0.9908
		NAWM	7.683±1.327			
		Lesion	8.380±1.091			
	1X LPS	Non-induced	8.138±2.185			
		NAWM	7.914±1.910			
		Lesion	8.587±1.933			
	4X LPS	Non-induced	8.383±2.878			
		NAWM	8.081±2.280			
		Lesion	8.707±3.002			

Regarding the chronic phase, representative images of the GFAP staining are presented in Figure 11A. As observed in Figure 11B, and from two-way ANOVA analysis (table 11), there is a significant increase in the total length of astrocytes in EAE animals when compared to the non-induced, both in the NAWM and lesion areas. Regarding the process thickness (Figure 11C) and the arbor complexity of GFAP+ astrocytes (within-subject effects - radius: $F(19,513)=244.655$, $p<0.0001$, radius*treatment: $F(38,513)=0.449$, $p=1.000$, radius*disease: $F(38,513)=1.407$, $p=0.317$, radius*treatment*disease: $F(76,513)=0.586$, $p=1.000$; between-subject effects – treatment: $F(2,27)=0.190$, $p=0.828$, disease: $F(2,27)=0.734$, $p=0.490$, treatment*disease: $F(4,27)=0.466$, $p=0.760$ (Figure 11D), no differences were observed between EAE and non-induced animals. In addition, none of the LPS pretreatment conditions appear to have an effect on all of these parameters.

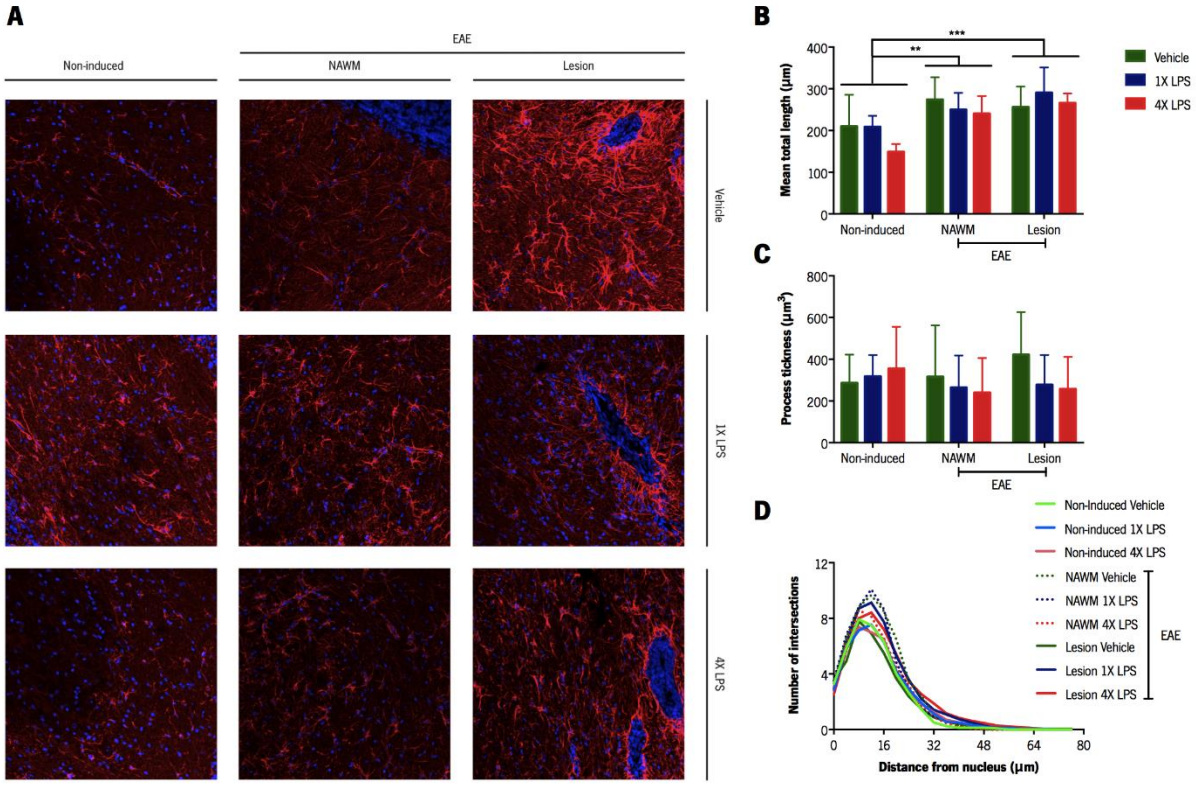

Figure 11 - GFAP immunohistochemical staining and morphological structure of astrocytes in the cerebellum at the chronic phase of the disease. Representative images from the cerebellum' white matter show the presence of astrogliosis in EAE animals (A). Characterization of the 3D structure of astrocytes by analysis of total length (B), process thickness (C) and sholl intersections (D) (Each animal corresponds to the mean of 6 astrocytes). **p<0.01, ***p<0.001.

Table 11 - Two-way ANOVA results of the total length and process thickness analysis of astrocytes in the cerebellum at the chronic phase of the disease.

			Mean±SEM	Disease factor	Treatment factor	Interaction
Total length	**Vehicle**	Non-induced	210.3±37.72	F (2,27) = 10.31, p = 0.0005	F (2,27) = 1.624, p = 0.2157	F (4,27) = 0.8635, p = 0.4984
		NAWM	274.2±26.73			
		Lesion	256.3±24.75			
	1X LPS	Non-induced	208.4±13.35			
		NAWM	249.7±20.39			
		Lesion	290.8±30.37			
	4X LPS	Non-induced	149.0±9.231			
		NAWM	240.8±20.86			
		Lesion	266.0±11.36			
Process thickness	**Vehicle**	Non-induced	286.2±68.10	F (2,27) = 0.2885, p = 0.7516	F (2,27) = 0.4256, p = 0.6577	F (2,28) = 0.5084, p = 0.7300
		NAWM	315.7±123.2			
		Lesion	421.6±102.4			
	1X LPS	Non-induced	317.7±51.16			
		NAWM	263.5±77.20			
		Lesion	277.6±71.37			
	4X LPS	Non-induced	354.5±100.30			
		NAWM	239.3±83.27			
		Lesion	257.3±77.03			

4. Discussion

In MS, the patient's immune system starts to attack the myelin sheath, leading to neuronal demyelination, neurodegeneration, and ultimately loss of vital neurological functions such as walking. There is no cure for MS and available treatments only slow down the initial-phases of the disease. This is partially due to the fact that later-disease mechanisms are poorly understood and do not directly correlate with the activity of immune system cells (the targets of available treatments). Rather, evidence suggests that disease progression and disability is better correlated with the maintenance of a low-grade persistent inflammation inside the CNS, driven by local glial cells (astrocytes and microglia) (Lassmann et al., 2012; Mahad et al., 2015). Specifically, microglia have recently emerged as a central player of innate immune memory in the CNS, a mechanism that was shown to be either beneficial or harmful to neuropathology, depending on the initial stimulus. These findings highlight the potential of microglia to be reprogrammed towards a more training or tolerant phenotype from outside the brain, which seems to be significant in MS disease, since it may open new possible therapeutic approaches. For that reason, in this thesis, we were interested in determine whether the training- (1X LPS) and tolerance-induced (4X LPS) peripheral stimulus could lead to long-term alterations in brain immune responses and thereby modify MS pathogenesis. In order to achieve that goal, we used the EAE mouse model, since it resembles the main histopathological and immunological features of MS (Bjelobaba et al., 2018), specifically in the C57BL/6 mice that develops a chronic disease course. In terms of clinical score, we showed that EAE disease course is not influenced by the LPS pretreatments. However, we found that EAE animals exposed to a training-induced stimulus (1X LPS) presented a significant delay in the appearance of the first symptoms. In terms of cerebellum' inflammatory profile and glial cells activation and structure, alterations in the expression levels of inflammatory cytokines and astrocytic activation markers were measured. Of interest, it was in the onset phase that we observed major alterations in terms of gene expression, where we found that *Il-6* and *Gfap* expression were higher in the training-LPS stimulation group. Of interest, although not statistically significant, the same tendency was observed, in the onset phase, for this experimental group, in the expression of *Il-12* and *Il-17*. However, only in the chronic phase this was translated in an increase in the lesioned area. Indeed, in terms of cerebellum lesioned area, we observed that in the onset phase no major differences were observed among groups, and that only at the chronic phase we have an increase in the percentage of lesioned area in the training-LPS stimulated group (1X LPS). No major alterations were observed in the expression level of the analyzed genes for the tolerance-LPS stimulation (4X LPS), neither in the lesioned area. Also, overall, no major alterations were observed in terms of astrocytic morphology between experimental groups.

4.1. Disease development upon peripheral stimulation with different LPS paradigms

In recent years, the concept of innate immune memory has emerged in the immunology field, becoming clear that cells of the innate immune system are also capable to retain memory. Since then, several *in vivo* and *in vitro* studies addressed this concept, providing insights on the innate memory characteristics, on the specific mechanisms underlying their effects, as well as in the impact on different pathologies. However, in the context of MS disease, the capacity of innate cells for long-lasting memory has not been tested yet. Nevertheless, the literature has already had some hints on the LPS pretreatment effects in EAE models (Buenafe & Bourdette, 2007; Ellestad et al., 2009). Namely, it is described that mice exposed to a single LPS injection early in life (2 weeks of age) and at 8 to 10 weeks of age and then induced with EAE 2-months or 72h later, respectively showed a delayed appearance of the first symptoms, although disease severity is only affected in animals treated at 2 weeks of age and induced with EAE 2-months later (Ellestad et al., 2009). In our work, even though peripheral stimulation with different LPS paradigms did not show any effects on disease severity, EAE animals exposed to a training-induced stimulus (1X LPS) presented a significant delay in the appearance of the first symptoms. However, we have to notice that animals exposed to a tolerance-induced stimulus (4X LPS), do not show any alterations in any disease-specific measures. This raises the question of whether the impact of LPS on EAE is variable depending on the concentration and timing of administration, which may play a critical role in the modulation of training/tolerant effects. We choose to perform the LPS injections 1-month before EAE induction because Wendeln et al. (2018) described that in an inducible focal brain ischemia disease model this timeframe was able to modulate microglia phenotype and consequently disease outcome. Even so, we recognize that EAE and stroke has different involvements of inflammation in their pathology, which increases the needs to carefully delineate the dose and timing of a stimulus in future studies. Unfortunately, herein we failed to observe that the tolerance-induced stimulus (4X LPS) was able to induce a decrease inflammatory response, as it was observed in the AD animal model and also in the stroke model.

Also, when comparing our study with those that injected LPS at 2 weeks and at 8 to 10 weeks of age and then induced EAE 2-months and 72h later, respectively, both studies used a protocol for EAE induction very similar to the one that we used. Specifically, the exception remains on the day of the second PTX injection, which was at day 1 in our case and at day 2 in both the other cases, and in the amount of PTX that was given, 100 ng per day in our experiment, while the other studies gave 75 ng in day 0 and 200 ng in day 2 (Ellestad et al., 2009), and 150 ng per day (Buenafe & Bourdette, 2007). But, although it is known that the amount of PTX that is given to the animals influences the severity of disease, since the

scores of our experiment and the scores of both Buenafe and Bourdette (2007) and Ellestad et al. (2009) experiments are similar, it does not appear to influence the development of the disease.

Overall, further studies are needed to fully understand the effects of innate immune memory in EAE disease development, since although the delayed effect observed in the appearance of the first symptoms in EAE animals exposed to a training-induced stimulus (1X LPS), this was not sufficient to have an impact on disease severity measured using the clinical score scale. Unfortunately, the clinical score scale not always represents the most accurate way to access disease severity and for that reason, although the previous result, we went further to dissect if the different LPS stimulations were playing a role in the molecular response.

4.2. Inflammation in the cerebellum of EAE animals

In the present work, we wanted to evaluate the impact of training- (1X LPS) and tolerance-induced stimulus (4X LPS) in EAE model. For that, we focused our attention in the cerebellum, which is a region commonly affected in this model, as well as in MS patients (Wilkins, 2017). The pathologic hallmark of MS is the formation of focal demyelinating plaques (Constantinescu et al., 2011), which can be found in the white matter of the cerebellum. Thus, we stained representative sections of the whole cerebellum of EAE animals with Luxol Fast Blue, and evaluated the percentage of area where we found clusters of infiltrating cells. At the onset phase of the disease, no significant alterations were observed among LPS pretreatment groups, opposing to what is observed during the chronic phase, where EAE animals exposed to a training-induced stimulus (1X LPS) presented a higher percentage of lesioned areas compared to EAE animals exposed to a tolerance-induced stimulus (4X LPS) and also compared to EAE control animals. Also, we have to notice that EAE animals exposed to a tolerance-induced stimulus (4X LPS) and EAE control animals presented a higher percentage of lesioned areas at the onset phase compared to the chronic phase, while EAE animals exposed to a training-induced stimulus (1X LPS) showed an increased percentage of lesioned areas at the chronic phase. These EAE control animals' results are in agreement to what was observed in a published work from our group (das Neves et al., 2018) that reports that EAE animals presented a significant decrease in the percentage of lesioned areas in the chronic phase, compared to the onset phase. Regarding the previous studies on LPS effects in EAE models, only Ellestad et al. (2009) that injected LPS at 2 weeks of age and induce EAE 2-months later, described loss of myelin staining in EAE animals, without differences among PBS- and LPS-exposed EAE animals.

In the analysis performed in our study, we should however highlight that the delimitation of lesioned areas in the two experiments (in the two disease timepoints) were performed with different software's but, the percentage of lesioned areas were calculated in the same way, so we do not expect that this will impact significantly in the results. To further confirm if the selected lesioned areas in the Luxol Fast Blue staining correspond to demyelination, an additional myelin marker, like FluoroMyelin or MOG itself, should be performed.

To understand what happens in the cerebellum at the molecular level, we next analyzed the expression levels of inflammation-associated genes. Because the importance of Th1 and Th17 cells in the etiology of MS, and even in EAE development has long been recognized (Sospedra & Martin, 2005) we analyzed Th1 and Th17 related cytokines. Indeed, we observed an increased expression of cytokines involved in Th1 immune response, namely *Ifn-gamma* and *Il-12*, and a cytokine involved in Th17 immune response, *Il-17*, in EAE animals at the onset phase of the disease. During the chronic phase, only the expression levels of *Ifn-gamma* and *Il-17* were significantly increased. Nevertheless, differences among LPS pretreatment groups were not observed for these cytokines in both disease phases. Ellestad et al. (2009), that injected LPS once at 2 weeks of age and then 2-months later induced EAE, showed similar results for the expression levels of *Ifn-gamma* in the spinal cord of EAE animals, at day 30 post-EAE induction.

The expression levels of *Il-6*, a multifunctional cytokine that is described as a promotor of EAE clinical manifestations (Samoilova et al., 1998), were observed to be significantly increased in the EAE animals compared to the non-induced in both disease phases. Nevertheless, at the onset phase, *Il-6* showed to be significantly more expressed in EAE animals exposed to a training-induced stimulus (1X LPS) when compared to EAE animals exposed to a tolerance-induced stimulus (4X LPS) and EAE control animals. In fact, previous studies described that in a cuprizone-induced demyelination model, astrocyte-targeted production of IL-6 significantly reduced demyelination, axonal damage, and astroglial and microglial activation in the corpus callosum (Petković, Campbell, Gonzalez, & Castellano, 2016), as well as reduced demyelination along with a chronically activated but less responsive microglia in the cerebellum (Petković, Campbell, Gonzalez, & Castellano, 2017). These findings may suggest a role for cell-specific IL-6 production in the modulation of training microglia phenotype with impact in the regulation of demyelination in EAE animals, which could also explain the results of the Luxol Fast Blue staining. Still, further studies are needed to disclose the molecular mechanisms involved in this process.

4.3. Activation of astrocytes and microglia in the cerebellum of EAE animals

The neuroinflammatory process present in EAE is characterized by the activation of microglia and astrocytes. This activation leads to the production of cytokines and chemokines that, in a chronic manner, may be deleterious to the brain (Sochocka et al., 2017). A new evidence reports that, in the brain, innate immune memory is predominantly mediated by microglia, which brings up possible contributions of this cell type and this mechanism in brain disorders with a strong inflammatory component, such as MS. Indeed, we observed an increased expression of genes related with microglia and astrocyte activation in EAE animals at both disease phases. Regarding astrocytes, from the genes analyzed, LPS pretreatment paradigms only influences the expression of *Gfap*, at the onset phase of disease, where EAE animals exposed to a training-induced stimulus (1X LPS) presented a higher expression of *Gfap* when compared to EAE animals exposed to a tolerance-induced stimulus (4X LPS) and when compared to EAE control animals. Interestingly, these results could be related to what was previously shown in the inflammation-related genes analysis, since *Il-6* exhibited the same pattern of expression. In fact, it is known from the literature that neurons, astrocytes, microglia and endothelial cells are the essential sources of IL-6 in the CNS (Erta, Quintana, & Hidalgo, 2012), which may suggests a role of astrocytes and IL-6 production in the mechanisms underlying EAE. In addition, recent studies shown that activated microglia induces reactive astrocytes in CNS disease and injury states (Liddelow et al., 2017), which raises the possible interplay of these cells on the mediation of innate immune memory in EAE. Therefore, a more thorough understanding of the downstream signaling pathways of IL-6 and their relation with EAE, can give us more information on the modulation of innate immune memory in the brain.

In terms of genes related with microglia activation, we have to notice that, at the onset phase of the disease, *Iba1*, *Cx3cr1*, *Mhc-II* and *inos* showed an increased expression in EAE animals compared to the non-induced while, during the chronic phase of the disease, these differences were only sustained in *Iba1*, *Cx3cr1* and *Mhc-II* genes. Nevertheless, we did not found any effect of the LPS pretreatment paradigms on the microglia-related genes analyzed. However, this does not mean that microglia were not reprogrammed by the LPS paradigms. Indeed, as we will refer further, additional measurements are needed to determine if LPS treatments are targeting the epigenetic and metabolic alterations that are associated with trained microglia (Wendeln et al., 2018). Also, as referred before, microglia and monocytes are difficult to distinguish, both morphologically and functionally and, indeed in our study the markers used did not discriminate between cells with a microglia or macrophage phenotype. This suggests that the effects evoked by microglia could be masked by the recruitment of additional myeloid cells from peripheral monocytes. Therefore, additional studies with the use of cell-specific markers

together with a spectrum of functional markers must be performed, not only for gene expression analysis, but also for the future analysis of the microglia stereological quantification. For that, a recent study on brain autopsy tissue from MS patients described the phenotypes of microglia and macrophages on staged lesions in acute, relapsing and progressive forms of disease using specific markers that characterize the origin and functional states of these cells (Zrzavy et al., 2017). Of interest, to determine microglia and macrophage phenotypes, they used Iba1 as a general marker, and to select microglia, they used transmembrane protein 119 (TMEM119) and purinergic receptor P2Y (P2RY12). In the brain, P2RY12 is specifically expressed in homeostatic microglia, since it was never observed on cells with a macrophage phenotype in MS lesions nor in the normal white matter of controls. However, the morphology of these cells does not allow us to distinguish the yolk sac-derived microglia from the recruited myeloid cells. To accomplish this, we have to use TMEM119, a recent marker that has been shown to discriminate resident microglia from recruited myeloid cells, both in experimental models and human brain tissue (Bennett et al., 2016; Satoh et al., 2016). Furthermore, as Bennett et al. (2016) described, it would be also interestingly to purify, by fluorescence-activated cell sorting, microglia from the brains of EAE animals previously exposed to LPS paradigms, and perform further mRNA analysis on these cells. Another possible direction remains on the mechanisms already described to be involved on the modulation of memory in innate immune cells (Domínguez-Andrés, Joosten, & Netea, 2019; Dominguez-Andres & Netea, 2018). As Wendeln et al. (2018) showed in the microglial gene expression analysis, the alterations observed among LPS pretreatment groups in an AD mouse model revealed striking parallels to epigenetic and metabolic changes. For example, 1X LPS-injected AD animals showed an increased expression of genes from modules enriched in HIF-1α signaling pathway and glycolysis pathway, while 4X LPS-injected AD animals showed a decreased expression of these genes. The role of cellular metabolism in the induction of innate immune memory has emerged in the recent years, and several studies already identify metabolic pathways involved on this mechanism, as previously referred. However, much more work has to be performed on this topic, namely to understand how to modulate these intracellular processes. Through the same analysis, Wendeln et al. (2018) showed a decreased expression of genes from a module enriched in phagocytosis-related pathways in AD control animals, and further decreased in 1X LPS-injected AD animals, but showed unchanged levels in 4X LPS-injected AD animals. These findings reflect the epigenetic alterations described for immune memory of innate cells. In the context of our work, different techniques could be applied to assess these mechanisms, and the previous suggestion of microglia isolation from the brains of EAE animals injected with LPS paradigms may open the horizons for some. For instance, since a shift of glucose metabolism from oxidative phosphorylation to glycolysis

resulting in more lactate production has been described in a trained macrophage, it would be interest to measure the release of lactate in microglial cells after LPS exposure in the context of EAE. Also, a chromatin immunoprecipitation assay could be performed in microglia, specifically to determine whether transcriptional alterations are behind their phenotype.

4.4. Astrogliosis in the cerebellum of EAE animals

As referred before, astrocytes are important players in the modulation of the neuroinflammatory response in MS and EAE (Brambilla, 2019). Therefore, in order to assess their structure in response to EAE under the influence of LPS paradigms, we stained cerebellum sections from each EAE group, and from each non-induced group as control, with GFAP, both at the onset and chronic phases of the disease. Posteriorly, z-stack confocal images of the cerebellum' white matter were taken, and astrocyte-specific structural features were assessed using the FIJI-Image J SNT plugin software. Additionally, in EAE animals, we analyzed both NAWM and lesioned areas.

At the onset phase of the disease, the analysis of the total length of astrocytes showed a decreased in both LPS groups (1X LPS and 4X LPS) when compared to all the vehicle groups, while at the chronic phase, an increased total length of astrocytes was observed in EAE animals when compared to the non-induced, both in NAWM and lesioned areas, but without differences among LPS treated animals. Those results suggested us that even in the absence of a CNS inflammatory process, LPS could have an effect in the activation of astrocytes. Also, those results suggested us that even in areas without clusters of infiltrating cells, astrocytes undergo morphological changes. Regarding the analysis of process thickness, no alterations were observed in EAE animals in comparison to the non-induced, at both disease phases, which deserves further clarification. In the sholl analysis, which gives us the arbor complexity of astrocytes, a decreased number of intersections was observed in both LPS groups (1X LPS and 4X LPS) when compared to all the vehicle groups, which is similar to what we observed in the astrocytic total length results at this phase of disease. At the chronic phase, no alterations in the arbor complexity of astrocytes were observed. Previous data on innate immune memory and astrocytes only referred that the number of $GFAP^+$ cells is decreased in 1X LPS-injected animals, compared to the PBS-injected controls (Wendeln et al., 2018). However, these was observed in an AD mouse model, which has a completely different inflammatory component, and was quantified in a plaque-associated area. Nevertheless, we have to keep in mind that these are two different ways to evaluate the process of activation of astrocytes, which is very complex and integrates both cell proliferation, morphological changes and functional modifications.

5. Concluding remarks

Until very recently, the capacity of a cell to retain memory was only attributed to the cells of the adaptive immune system. However, recent findings introduced innate immune cells as also capable of retaining memory (Netea et al., 2011; Töpfer et al., 2015), and specifically microglia seems to be the predominant mediator of innate immune memory in the brain (Wendeln et al., 2018). In the context of MS, the capacity of innate cells for long-lasting memory has never been tested. Therefore, in the present work, we disclosed some of the outcomes observed in an EAE mouse model upon peripheral stimulation with different LPS paradigms.

Our findings identify a delayed effect in the appearance of the first symptoms in EAE animals exposed to a training-induced stimulus (1X LPS), suggesting a role for acute immune training in disease establishment. However, these effects deserve further investigation not only because they were observed only in one of the two experiments, but especially because it was observed that EAE animals exposed to this training-induced stimulus (1X LPS) expressed more *Il-6* at the onset phase of disease, and presented a higher percentage of lesioned area during the chronic phase of disease. Also, we found higher expression of *Gfap* in EAE animals exposed to a training-induced stimulus (1X LPS), at the onset phase of disease. These results indicate that, indeed, the training-induced stimulus (1X LPS) is able to be deleterious, at least in specific EAE outcomes that we analyzed. In addition, no alterations were observed when analyzing the animals submitted to the tolerance-induced stimulus (4 X LPS), where we expected to have a protective effect due to the fact that, tolerant microglia was shown to be able to decrease brain inflammation in other pathologies.

Despite the fact that no significant differences were observed in microglia-related genes, among LPS pretreatment groups, this does not seem sufficient to conclude that peripheral inflammatory stimulus has not exert long-term alterations in the brain. Further studies using specific markers that characterize the origin and functional states of microglia are remarkably needed, as well as the assessment of specific metabolites and signaling molecules involved in the metabolic and epigenetic reprogramming of these cells.

Overall, this work suggests that modulation of CNS-resident innate immune cells memory may play a role in disease pathology (at least the training stimulation). However, the tolerance-induced phenotype was not able to delay or ameliorate EAE phenotype but, we have to keep in mind that, being MS characterized by an exacerbated immune response, the peripheral inflammatory stimulus that we gave to the animals, may not be enough to counterbalance the ability to respond to disease. Therefore, further investigation

on the mechanisms behind this acute immune training and acute immune tolerance in EAE model is needed.

Bibliography

Ajami, B., Samusik, N., Wieghofer, P., Ho, P. P., et al. (2018). Single-cell mass cytometry reveals distinct populations of brain myeloid cells in mouse neuroinflammation and neurodegeneration models. *Nature Neuroscience*, *21*(4), 541–551. doi:10.1038/s41593-018-0100-x

Arts, R. J. W., Joosten, L. A. B., & Netea, M. G. (2016). Immunometabolic circuits in trained immunity. *Seminars in Immunology*, *28*(5), 425–430. doi:10.1016/j.smim.2016.09.002

Awate, S., Babiuk, L. A., & Mutwiri, G. (2013). Mechanisms of action of adjuvants. *Frontiers in Immunology*, *4*(114), 1–10. doi:10.3389/fimmu.2013.00114

Barnett, M. H., & Prineas, J. W. (2004). Relapsing and Remitting Multiple Sclerosis: Pathology of the Newly Forming Lesion. *Annals of Neurology*, *55*(4), 458–468. doi:10.1002/ana.20016

Baxter, A. G. (2007). The origin and application of experimental autoimmune encephalomyelitis. *Nature Reviews Immunology*, *7*(11), 904–912. doi:10.1038/nri2190

Bennett, M. L., Bennett, F. C., Liddelow, S. A., Ajami, B., et al. (2016). New tools for studying microglia in the mouse and human CNS. *Proceedings of the National Academy of Sciences of the United States of America*, *113*(12), 1738–1746. doi:10.1073/pnas.1525528113

Bittner, S., Afzali, A. M., Wiendl, H., & Meuth, S. G. (2014). Myelin Oligodendrocyte Glycoprotein (MOG35-55) Induced Experimental Autoimmune Encephalomyelitis (EAE) in C57BL/6 Mice. *Journal of Visualized Experiments*, (86), e51275. doi:10.3791/51275

Bjelobaba, I., Begovic-Kupresanin, V., Pekovic, S., & Lavrnja, I. (2018). Animal models of multiple sclerosis: Focus on experimental autoimmune encephalomyelitis. *Journal of Neuroscience Research*, *96*(6), 1021–1042. doi:10.1002/jnr.24224

Bodea, L.-G., Wang, Y., Linnartz-Gerlach, B., Kopatz, J., et al. (2014). Neurodegeneration by Activation of the Microglial Complement-Phagosome Pathway. *Journal of Neuroscience*, *34*(25), 8546–8556. doi:10.1523/jneurosci.5002-13.2014

Bogie, J. F. J., Stinissen, P., & Hendriks, J. J. A. (2014). Macrophage subsets and microglia in multiple sclerosis. *Acta Neuropathologica*, *128*(2), 191–213. doi:10.1007/s00401-014-1310-2

Brambilla, R. (2019). The contribution of astrocytes to the neuroinflammatory response in multiple sclerosis and experimental autoimmune encephalomyelitis. *Acta Neuropathologica*, *137*(5), 757–783. doi:10.1007/s00401-019-01980-7

Browne, P., Tremlett, H., Baker, C., & Taylor, B. V. (2014). Atlas of Multiple Sclerosis 2013: A growing global poblem with widespread inequity. *American Academy of Neurology*, *83*(11), 1022–1024.

Bruck, W., Porada, P., Poser, S., Rieckmann, P., et al. (1995). Monocyte/Macrophage Differentiation in Early Multiple Sclerosis Lesions. *Annals of Neurology*, *38*(5), 788–796. doi:10.1002/ana.410380514

Buenafe, A. C., & Bourdette, D. N. (2007). Lipopolysaccharide pretreatment modulates the disease course in experimental autoimmune encephalomyelitis. *Journal of Neuroimmunology*, *182*(1–2), 32–40. doi:10.1016/j.jneuroim.2006.09.004

Butovsky, O., Jedrychowski, M. P., Moore, C. S., Cialic, R., et al. (2014). Identification of a unique TGF-β-dependent molecular and functional signature in microglia. *Nature Neuroscience*, *17*(1), 131–143. doi:10.1038/nn.3599

Cao, L., & He, C. (2013). Polarization of macrophages and microglia in inflammatory demyelination. *Neuroscience Bull*, *29*(2), 189–198. doi:10.1007/s12264-013-1324-0

Carey, B. W., Finley, L. W. S., Cross, J. R., Allis, C. D., & Thompson, C. B. (2015). Intracellular α-ketoglutarate maintains the pluripotency of embryonic stem cells. *Nature*, *518*(7539), 413–416. doi:10.1038/nature13981

Christ, A., Bekkering, S., Latz, E., & Riksen, N. P. (2016). Long-term activation of the innate immune system in atherosclerosis. *Seminars in Immunology*, *28*(4), 384–393. doi:10.1016/j.smim.2016.04.004

Compston, A., & Coles, A. (2008). Multiple sclerosis. *The Lancet*, *372*(9648), 1502–1517. doi:10.1016/S0140-6736(08)61620-7

Constantinescu, C. S., Farooqi, N., O'Brien, K., & Gran, B. (2011). Experimental autoimmune encephalomyelitis (EAE) as a model for multiple sclerosis (MS). *British Journal of Pharmacology*, *164*(4), 1079–1106. doi:10.1111/j.1476-5381.2011.01302.x

Correale, J., Gaitán, M. I., Ysrraelit, M. C., & Fiol, M. P. (2016). Progressive multiple sclerosis : from pathogenic mechanisms to treatment multiple sclerosis. *Brain*, *140*(3), 527–546. doi:10.1093/brain/aww258

Crisan, T. O., Netea, M. G., & Joosten, L. A. B. (2016). Innate immune memory: Implications for host responses to damage-associated molecular patterns. *European Journal of Immunology*, *46*(4), 817–828. doi:10.1002/eji.201545497

das Neves, S. P., Serre-Miranda, C., Nobrega, C., Roque, S., et al. (2018). Immune Thymic Profile of the MOG-Induced Experimental Autoimmune Encephalomyelitis Mouse Model. *Frontiers in Immunology*, *9*(2335), 1–11. doi:10.3389/fimmu.2018.02335

Dendrou, C. A., Fugger, L., & Friese, M. A. (2015). Immunopathology of multiple sclerosis. *Nature Reviews Immunology*, *15*(9), 545–558. doi:10.1038/nri3871

Denica, A., Johnsonb, A. J., Bieberc, A. J., Warringtonc, A. E., et al. (2011). The Relevance of Animal Models in Multiple Sclerosis Research. *Pathophysiology*, *18*(1), 1–16. doi:10.1016/j.pathophys.2010.04.004.The

Domingues, H. S., Mues, M., Lassmann, H., Wekerle, H., & Krishnamoorthy, G. (2010). Functional and pathogenic differences of Th1 and Th17 cells in experimental autoimmune encephalomyelitis. *PLoS ONE*, *5*(11), 1–13. doi:10.1371/journal.pone.0015531

Domínguez-Andrés, J., Joosten, L. A., & Netea, M. G. (2019). Induction of innate immune memory: the role of cellular metabolism. *Current Opinion in Immunology*, *56*, 10–16. doi:10.1016/j.coi.2018.09.001

Dominguez-Andres, J., & Netea, M. G. (2018). Long-term reprogramming of the innate immune system. *Journal of Leukocyte Biology*, *105*(2), 329–338. doi:10.1002/JLB.MR0318-104R

Ellestad, K. K., Tsutsui, S., Noorbakhsh, F., Warren, K. G., et al. (2009). Early Life Exposure to Lipopolysaccharide Suppresses Experimental Autoimmune Encephalomyelitis by Promoting Tolerogenic Dendritic Cells and Regulatory T Cells. *The Journal of Immunology*, *183*(1), 298–309. doi:10.4049/jimmunol.0803576

Erta, M., Quintana, A., & Hidalgo, J. (2012). Interleukin-6, a major cytokine in the central nervous system.

International Journal of Biological Sciences, *8*(9), 1254–1266. doi:10.7150/ijbs.4679

Fang, M., Yamasaki, R., Li, G., Masaki, K., et al. (2018). Connexin 30 Deficiency Attenuates Chronic but Not Acute Phases of Experimental Autoimmune Encephalomyelitis Through Induction of Neuroprotective Microglia. *Frontiers in Immunology*, *9*(2588), 1–19. doi:10.3389/fimmu.2018.02588

Fazio, A. L. P., Fredrikson, S., & Granieri, E. (2010). The first case history of multiple sclerosis: Augustus d'Esté. *Neurological Sciences*, *31*(1), 29–33. doi:10.1007/s10072-009-0161-4

Gandhi, R., Laroni, A., & Weiner, H. L. (2011). Role of the innate immune system in the pathogenesis of multiple sclerosis. *Journal of Neuroimmunology*, *221*(1–2), 7–14. doi:10.1016/j.jneuroim.2009.10.015

Ghasemi, N., Razavi, S., & Nikzad, E. (2017). Multiple sclerosis: Pathogenesis, symptoms, diagnoses and cell-based therapy. *Cell Journal*, *19*(1), 1–10. doi:10.22074/cellj.2016.4867

Giunti, D., Parodi, B., Cordano, C., & De, N. K. (2014). Can we switch microglia ' s phenotype to foster neuroprotection ? Focus on multiple sclerosis. *British Society for Immunology*, *141*(3), 328–339. doi:10.1111/imm.12177

Glatigny, S., & Bettelli, E. (2018). Experimental autoimmune encephalomyelitis (EAE) as Animal Models of Multiple Sclerosis (MS). *Cold Spring Harbor Perspectives in Medicine*, *8*(11), 1–19. doi:10.1101/cshperspect.a028977

Goldenberg, M. M. (2012). Multiple Sclerosis Review. *P&T*, *37*(3), 175–184.

Gourbal, B., Pinaud, S., Beckers, G. J. M., Van Der Meer, J. W. M., et al. (2018). Innate immune memory: An evolutionary perspective. *Immunological Reviews*, *283*(1), 21–40. doi:10.1111/imr.12647

Greve, W., Enzmann, D., & Hosser, D. (2014). The presence of oligoclonal IgG bands in human CSF during the course of neurological diseases. *Journal of Neurology*, *261*(3), 554–560. doi:10.1007/s00415-013-7234-2

Haley, M. J., Brough, D., Quintin, J., & Allan, S. M. (2017). Microglial priming as trained immunity in the brain. *Neuroscience*, *1*(405), 47–54. doi:10.1016/j.neuroscience.2017.12.039

Hemmer, B., Archelos, J. J., & Hartung, H. (2002). New concepts in the immunopathogenesis of Multiple Sclerosis. *Nature Reviews Neuroscience*, *3*(4), 291–301. doi:10.1038/nrn784

Hemmer, B., Kerschensteiner, M., & Korn, T. (2015). Role of the innate and adaptive immune responses in the course of multiple sclerosis. *The Lancet Neurology*, Vol. 14. doi:10.1016/S1474-4422(14)70305-9

Ifrim, D. C., Quintin, J., Joosten, L. A. B., Jacobs, C., et al. (2014). Trained immunity or tolerance: Opposing functional programs induced in human monocytes after engagement of various pattern recognition receptors. *Clinical and Vaccine Immunology*, *21*(4), 534–545. doi:10.1128/CVI.00688-13

Italiani, P., & Boraschi, D. (2017). Induction of Innate Immune Memory by Engineered Nanoparticles: A Hypothesis That May Become True. *Frontiers in Immunology*, *8*(734), 1–6. doi:10.3389/fimmu.2017.00734

Jha, A. K., Huang, S. C. C., Sergushichev, A., Lampropoulou, V., et al. (2015). Network integration of

parallel metabolic and transcriptional data reveals metabolic modules that regulate macrophage polarization. *Immunity*, *42*(3), 419–430. doi:10.1016/j.immuni.2015.02.005

Keren-Shaul, H., Spinrad, A., Weiner, A., Matcovitch-Natan, O., et al. (2017). A Unique Microglia Type Associated with Restricting Development of Alzheimer's Disease. *Cell*, *169*(7), 1276–1290. doi:10.1016/j.cell.2017.05.018

Krasemann, S., Madore, C., Cialic, R., Baufeld, C., et al. (2017). The TREM2-APOE Pathway Drives the Transcriptional Phenotype of Dysfunctional Microglia in Neurodegenerative Diseases. *Immunity*, *47*(3), 566–581. doi:10.1016/j.immuni.2017.08.008

Labzin, L. I., Heneka, M. T., & Latz, E. (2018). Innate Immunity and Neurodegeneration. *Annual Review of Medicine*, *69*, 437–449. doi:10.1146/annurev-med-050715-104343

Larochelle, C., Alvarez, J. I., & Prat, A. (2011). How do immune cells overcome the blood-brain barrier in multiple sclerosis? *FEBS Letters*, *585*(23), 3770–3780. doi:10.1016/j.febslet.2011.04.066

Lassmann, H., & Bradl, M. (2017). Multiple sclerosis: experimental models and reality. *Acta Neuropathologica*, *133*(2), 223–244. doi:10.1007/s00401-016-1631-4

Lassmann, H., Horssen, J. van, & Mahad, D. (2012). Progressive multiple sclerosis: pathology and pathogenesis. *Nature Reviews Neurology*, *8*(11), 647–656. doi:10.1038/nrneurol.2012.168

Liddelow, S. A., Guttenplan, K. A., Clarke, L. E., Bennett, F. C., et al. (2017). Neurotoxic reactive astrocytes are induced by activated microglia. *Nature*, *541*(7638), 481–487. doi:10.1038/nature21029

Liu, T. F., Vachharajani, V. T., Yoza, B. K., & McCall, C. E. (2012). NAD+ -dependent sirtuin 1 and 6 proteins coordinate a switch from glucose to fatty acid oxidation during the acute inflammatory response. *Journal of Biological Chemistry*, *287*(31), 25758–25769. doi:10.1074/jbc.M112.362343

Loma, I., & Heyman, R. (2011). Multiple Sclerosis: Pathogenesis and Treatment. *Current Neuropharmacology*, *9*(3), 409–416. doi:10.2174/157015911796557911

Mahad, D. H., Trapp, B. D., & Lassmann, H. (2015). Pathological mechanisms in progressive multiple sclerosis. *The Lancet Neurology*, *14*(2), 183–193. doi:10.1016/S1474-4422(14)70256-X

Marcus, J. F., & Waubant, E. L. (2013). Updates on Clinically Isolated Syndrome and Diagnostic Criteria for Multiple Sclerosis. *The Neurohospitalist*, *3*(2), 65–80. doi:10.1177/1941874412457183

Marik, C., Felts, P. A., Bauer, J., Lassmann, H., & Smith, K. J. (2007). Lesion genesis in a subset of patients with multiple sclerosis: A role for innate immunity? *Brain*, *130*(11), 2800–2815. doi:10.1093/brain/awm236

Marques, F., Mesquita, S. D., Sousa, J. C., Coppola, G., et al. (2012). Lipocalin 2 is present in the EAE brain and is modulated by natalizumab. *Frontiers in Cellular Neuroscience*, *6*(33), 1–10. doi:10.3389/fncel.2012.00033

McKenzie, B. A., Mamik, M. K., Saito, L. B., Boghozian, R., et al. (2018). Caspase-1 inhibition prevents glial inflammasome activation and pyroptosis in models of multiple sclerosis. *Proceedings of the National Academy of Sciences*, *115*(26), 6065–6074. doi:10.1073/pnas.1722041115

Mecha, M., Carrillo-Salinas, F. J., Mestre, L., Feliú, A., & Guaza, C. (2013). Viral models of multiple

sclerosis: Neurodegeneration and demyelination in mice infected with Theiler's virus. *Progress in Neurobiology*, *101–102*(1), 46–64. doi:10.1016/j.pneurobio.2012.11.003

Miljković, D., & Spasojević, I. (2013). Multiple Sclerosis: molecular mechanisms and therapeutic opportunities. *Antioxidants & Redox Signaling*, *19*(18), 2286–2334. doi:10.1089/ars.2012.5068

Miller, D. H., Chard, D. T., & Ciccarelli, O. (2012). Clinically isolated syndromes. *The Lancet Neurology*, *11*(2), 157–169. doi:10.1016/S1474-4422(11)70274-5

Mills, E., & O'Neill, L. A. J. (2014). Succinate: a metabolic signal in inflammation. *Trends in Cell Biology*, *24*(5), 313–320. doi:10.1016/j.tcb.2013.11.008

Morris, M. C., Gilliam, E. A., & Li, L. (2014). Innate immune programing by endotoxin and its pathological consequences. *Frontiers in Immunology*, *5*(680), 1–8. doi:10.3389/fimmu.2014.00680

Netea, M. G., Joosten, L. A. B., Latz, E., Mills, K. H. G., et al. (2016). Trained immunity: a program of innate immune memory in health and disease. *Science*, *352*(6284), 1–23. doi:10.1126/science.aaf1098

Netea, M. G., Latz, E., Mills, K. H. G., & Neill, L. A. J. O. (2015). Innate immune memory: a paradigm shift in understanding host defense. *Nature Publishing Group*, *16*(7), 675–679. doi:10.1038/ni.3178

Netea, M. G., Quintin, J., & Van Der Meer, J. W. M. (2011). Trained immunity: A memory for innate host defense. *Cell Host and Microbe*, *9*(5), 355–361. doi:10.1016/j.chom.2011.04.006

O'Loughlin, E., Madore, C., Lassmann, H., & Butovsky, O. (2018). Microglial phenotypes and functions in multiple sclerosis. *Cold Spring Harbor Perspectives in Medicine*, *8*(2), 1–22. doi:10.1101/cshperspect.a028993

Otto Warburg, B., Wind, F., & Negelein, N. (1927). The metabolism of tumours in the body. *The Journal of General Physiology*, *8*(6), 519–530.

Our, S. (2013). Atlas of MS. In *Multiple Sclerosis International Federation*.

Palmer, C. S., Henstridge, D. C., Yu, D., Singh, A., et al. (2016). Emerging Role and Characterization of Immunometabolism: Relevance to HIV Pathogenesis, Serious Non-AIDS Events, and a Cure. *The Journal of Immunology*, *196*(11), 4437–4444. doi:10.4049/jimmunol.1600120

Peferoen, L., Kipp, M., van der Valk, P., van Noort, J. M., & Amor, S. (2014). Oligodendrocyte-microglia cross-talk in the central nervous system. *British Society for Immunology*, *141*(3), 302–313. doi:10.1111/imm.12163

Petković, F., Campbell, I. L., Gonzalez, B., & Castellano, B. (2016). Astrocyte-targeted production of interleukin-6 reduces astroglial and microglial activation in the cuprizone demyelination model: Implications for myelin clearance and oligodendrocyte maturation. *Glia*, *64*(12), 2104–2119. doi:10.1002/glia.23043

Petković, F., Campbell, I. L., Gonzalez, B., & Castellano, B. (2017). Reduced cuprizone-induced cerebellar demyelination in mice with astrocyte-targeted production of IL-6 is associated with chronically activated, but less responsive microglia. *Journal of Neuroimmunology*, *310*, 97–102. doi:10.1016/j.jneuroim.2017.07.003

Piccio, L., Buonsanti, C., Mariani, M., Cella, M., et al. (2007). Blockade of TREM-2 exacerbates

experimental autoimmune encephalomyelitis. *European Journal of Immunology*, *37*(5), 1290–1301. doi:10.1002/eji.200636837

Popescu, B. F. G., Pirko, I., & Lucchinetti, C. F. (2013). Pathology of multiple sclerosis: Where do we stand? *CONTINUUM: Lifelong Learning in Neurology*, *19*(4), 901–921. doi:10.1212/01.CON.0000433291.23091.65

Püntener, U., Booth, S. G., Perry, V. H., & Teeling, J. L. (2012). Long-term impact of systemic bacterial infection on the cerebral vasculature and microglia. *Journal of Neuroinflammation*, *9*(146), 1–13. doi:10.1186/1742-2094-9-146

Ransohoff, R. M. (2012). Animal models of multiple sclerosis : the good , the bad and the bottom line. *Nature Neuroscience*, *15*(8), 1074–1077. doi:10.1038/nn.3168

Rinchai, D., Boughorbel, S., Presnell, S., Quinn, C., & Chaussabel, D. (2016). A curated compendium of monocyte transcriptome datasets of relevance to human monocyte immunobiology research. *F1000Research*, *5*(291), 1–18. doi:10.12688/f1000research.8182.1

Saeed, S., Quintin, J., Kerstens, H. H. D., Rao, N. A., et al. (2014). Epigenetic programming during monocyte to macrophage differentiation and trained innate immunity. *Science*, *345*(6204), 1–26. doi:10.1126/science.1251086

Salam, A. P., Borsini, A., & Zunszain, P. A. (2017). Trained innate immunity: a salient factor in the pathogenesis of neuroimmune psychiatric disorders. *Molecular Psychiatry*, *23*(2), 170–176. doi:10.1038/mp.2017.186

Salam, Alex P, Pariante, C. M., & Zunszain, P. (2017). Innate Immune Memory: Implications for Microglial Function and Neuroprogression. *Modern Trends in Pharmacopsychiatry*, *31*, 67–78. doi:10.1159/000470808

Samoilova, E. B., Horton, J. L., Hilliard, B., Liu, T.-S. T., & Chen, Y. (1998). IL-6-Deficient Mice Are Resistant to Experimental Autoimmune Encephalomyelitis: Roles of IL-6 in the Activation and Differentiation of Autoreactive T Cells. *The Journal of Immunology*, *161*(12), 6480–6486.

Sankowski, R., Mader, S., & Valdés-Ferrer, S. I. (2015). Systemic Inflammation and the brain: novel roles of genetic, molecular, and environmental cues as drivers of neurodegeneration. *Frontiers in Cellular Neuroscience*, *9*(28), 1–20. doi:10.3389/fncel.2015.00028

Satoh, J. ichi, Kino, Y., Asahina, N., Takitani, M., et al. (2016). TMEM119 marks a subset of microglia in the human brain. *Neuropathology*, *36*(1), 39–49. doi:10.1111/neup.12235

Seeley, J. J., Baker, R. G., Mohamed, G., Bruns, T., et al. (2018). Induction of innate immune memory via microRNA targeting of chromatin remodelling factors. *Nature*, *559*, 114–119. doi:10.1038/s41586-018-0253-5

Shemer, A., Erny, D., Jung, S., & Prinz, M. (2015). Microglia Plasticity During Health and Disease: An Immunological Perspective. *Trends in Immunology*, *36*(10), 614–624. doi:10.1016/j.it.2015.08.003

Shi, L., Eugenin, E. A., & Subbian, S. (2016). Immunometabolism in tuberculosis. *Frontiers in Immunology*, *7*(150), 1–15. doi:10.3389/fimmu.2016.00150

Sochocka, M., Diniz, B. S., & Leszek, J. (2017). Inflammatory Response in the CNS: Friend or Foe ? *Molecular Neurobiology*, *54*(10), 8071–8089. doi:10.1007/s12035-016-0297-1

Sosa, R. A., Murphey, C., Cardona, A. E., Ji, N., & Forsthuber, T. G. (2013). The Kinetics of Myelin Antigen Uptake by Myeloid Cells in the Central Nervous System during Experimental Autoimmune Encephalomyelitis. *The Journal of Immunology*, *191*(12), 5848–5857. doi:10.4049/jimmunol.1300771

Sospedra, M., & Martin, R. (2005). Immunology of Multiple Sclerosis. *Annual Review of Immunology*, *23*, 683–747. doi:10.1146/annurev.immunol.23.021704.115707

Tavares, G., Martins, M., Correia, J. S., Sardinha, V. M., et al. (2017). Employing an open-source tool to assess astrocyte tridimensional structure. *Brain Structure and Function*, *222*(4), 1989–1999. doi:10.1007/s00429-016-1316-8

Thompson, A. J., Banwell, B. L., Barkhof, F., Carroll, W. M., et al. (2018). Diagnosis of multiple sclerosis: 2017 revisions of the McDonald criteria. *The Lancet Neurology*, *17*(2), 162–173. doi:10.1016/S1474-4422(17)30470-2

Thompson, K. K., & Tsirka, S. E. (2017). The Diverse Roles of Microglia in the Neurodegenerative Aspects of Central Nervous System (CNS) Autoimmunity. *International Journal of Molecular Sciences*, *18*(3), 1–15. doi:10.3390/ijms18030504

Töpfer, E., Boraschi, D., & Italiani, P. (2015). Innate Immune Memory: The Latest Frontier of Adjuvanticity. *Journal of Immunology Research*, *2015*, 1–7. doi:10.1155/2015/478408

Voet, S., Mc Guire, C., Hagemeyer, N., Martens, A., et al. (2018). A20 critically controls microglia activation and inhibits inflammasome-dependent neuroinflammation. *Nature Communications*, *9*(1), 1–15. doi:10.1038/s41467-018-04376-5

Weiner, H. L. (2008). A shift from adaptive to innate immunity: A potential mechanism of disease progression in multiple sclerosis. *Journal of Neurology*, *255*(1), 3–11. doi:10.1007/s00415-008-1002-8

Wendeln, A. C., Degenhardt, K., Kaurani, L., Gertig, M., et al. (2018). Innate immune memory in the brain shapes neurological disease hallmarks. *Nature*, *556*(7701), 332–338. doi:10.1038/s41586-018-0023-4

Wilkins, A. (2017). Cerebellar Dysfunction in Multiple Sclerosis. *Frontiers in Neurology*, *8*(312), 1–6. doi:10.3389/fneur.2017.00312

Yoshida, K., Maekawa, T., Zhu, Y., Renard-Guillet, C., et al. (2015). The transcription factor ATF7 mediates lipopolysaccharide-induced epigenetic changes in macrophages involved in innate immunological memory. *Nature Immunology*, *16*(10), 1034–1043. doi:10.1038/ni.3257

Zrzavy, T., Hametner, S., Wimmer, I., Butovsky, O., et al. (2017). Loss of 'homeostatic' microglia and patterns of their activation in active multiple sclerosis. *Brain*, *140*(7), 1900–1913. doi:10.1093/brain/awx113

Annex 1 – DNA sequences of the primers used in qRT-PCR.

Mouse cDNAs	Primer sequences	GenBank™ accession number	Annealing temperature (°C)
Atp5b	Fw 5' GGC CAA GAT GTC CTG CTG TT 3' Rv 5' GCT GGT AGC CTA CAG CAG AAG G 3'	NM_016774.3	60
Hspcb	Fw 5' GCT GGC TGA GGA CAA GGA GA 3' Rv 5'CGT CGG TTA GTG GAA TCT TCA TG 3'	NM_008302.3	60
Ifn-gamma	Fw 5' ACT GGC AAA AGG ATG GTG AC 3' Rv 5' TGA GCT CAT TGA ATG CTT GG 3'	NM_008337.3	58
Il-12	Fw 5' GTG TCT TAG CCA GTC CCG AA 3' Rv 5' TTC AAG TCC TCA TAG ATG CTA CCA A 3'	NM_008351.3	59
Il-17	Fw 5' GGA CTC TCC ACC GCA ATG AA 3' Rv 5' CAT GTG GTG CTC CAG CTT TC 3'	NM_010552.3	58
Il-4	Fw 5'GTC ACA GGA GAA GGG ACG CCA T 3' Rv 5'AGC CCT ACA GAC GAG CTC ACT C 3'	NM_021283.2	58
Il-6	Fw 5' CCG GAG AGG AGA CTT CAC AG 3' Rv 5' TCC ACG ATT TCC GAG AGA AC 3'	NM_031168.2	59
Gfap	Fw 5' AACCGCATCACCATTCCTGT 3' Rv 5' TCCTTAATGACCTCGCCATCC 3'	XR_388347.2	60
Lcn2	Fw 5'CCA GTT CGC CAT GGT ATT TT 3' Rv 5' GGT GGG GAC AGA GAA GAT GA 3'	NM_008491.1	58
Iba1	Fw 5' GAA GCG AAT GCT GGA GAA AC 3' Rv 5' CTC ATA CAT CAG AAT CAT TCT C 3'	NM_001361501.1	60
Cx3cr1	Fw 5'CGT CGA GAC TGG GTG AGT GAC 3' RV 5'AAG GAG GTG GAC GAC ATG GTG AG 3'	NM_009987.4	60
Mhc-II	Fw 5'GAG CAT CCC AGC CTG AAG A 3' Rv 5'CGA TGC CGC TCA ACA TCT T 3'	NM_207105.3	60
inos	Fw 5'CTC GGA GGT TCA CCT CAC TGT 3' Rv 5' GCT GGA AGC CAC TGA CAC TT 3'	NM_010927.4	59